

# **Proposal to Study the Feasibility to Site Various Neutrino Detectors at WIPP for Neutrino Factories or Superbeams**

D.B. Cline, K. Lee, P.F. Smith, and B. Lisowski  
*University of California Los Angeles*

R.F. Burkart, W. Burgett and E.J. Fenyves  
*University of Texas Dallas*

K. McDonald and C. Lu  
*Princeton, Experimental High Energy Physics, Department of Physics*

Franco Sergiampietri and C.Cerri  
*INFN-Sezione di Pisa, Italy*

J. Learned  
*University of Hawaii*

*Waste Isolation Pilot Plant*

N. Elkins  
*LANL and Sandia (Carlsbad)*

## **1.1 Prologue**

The following statement from the Snowmass 2001 conference is the draft consensus statement of the E1 working group and is reproduced in its entirety:

"The recent discovery of neutrino oscillations is the first confirmed physics beyond the Standard Model and strongly suggests a new fundamental energy scale. Accordingly, the US should strengthen its lepton flavor research program by expediting construction of a high-intensity, conventional neutrino beam (a 'superbeam').

"A superbeam will probe the neutrino mixing angles and mass hierarchy and may discover leptonic CP violation. The full program will require neutrino beams of multiple energies and massive detectors at multiple baselines. The facilities will also support a rich program of other physics, including proton decay, particle astrophysics and lepton flavor violating processes.

"A superbeam facility builds the foundation for a future muon-based neutrino source (a 'neutrino factory') with even greater physics potential. The development of the needed technology requires a dedicated R&D effort in which the US should be a strong partner".

## 1.2 Introduction

In 1932, a young Wolfgang Pauli proposed to the Solway conference that the electron energy spectra measured by Bray from the Uranium radioactive decay could be explained with the introduction of a new particle that he called 'Neutrino' as an invisible particle. In 1950 a solar neutrino experiment began in the Homestake gold mine in South Dakota [ref\_RayDavis], and with it began a new intensity of interest in neutrino research, which continues to the present. As early as in 1938, the p-p solar energy production mechanisms was worked out by Bethe and others based upon the initial reactions of hydrogen nuclei combining to give deuterium and helium nuclei, with the additional production of large amounts of energy and neutrinos. By 1939, the CNO cycle was added. Detailed solar models soon followed which predicted the solar neutrino flux striking the earth. When the Homestake data was analyzed, it was found that less than half of the predicted neutrinos had been detected; and so began the last thirty years of intensive neutrino study. These studies have involved solar, atmospheric (from cosmic rays), reactor, and accelerator neutrinos.

The neutrino's nonreactive nature has made it an experimentally elusive particle, and thus much basic information on neutrino physics is still missing. New experiments now planned or under construction, both near and long term, hope to gather the additional experimental evidence needed to refine this particle's place in the standard model. These experiments expect to benefit from having larger detectors, and from having new sources of high-energy neutrino beams. One such source under consideration is a neutrino factory, producing large quantities of neutrinos from the decay of muons in a storage ring and directing these neutrinos to distant detectors. The advantages of the neutrino factory and detector combination for unlocking new physics rest upon the neutrino factory's high beam intensity, its composition, energy range, and uniformity, and the relatively long distances possible between the factory and the detector.

Neutrino oscillation has been an important topic of study recently in the astrophysics and particle physics fields since the first announcement of its evidence in 1996 by the 50 kton water Cerenkov detector Super-Kamiokande (Super-K). Over the last five years, the experiment continued to collect more data on the solar neutrinos and the cosmic muon-atmospheric neutrinos at the same time functions as an observatory for neutrino bursts from gravitational collapse as 1987A supernova that occurred in the Large Magellanic Cloud on the outer edge of our galaxy. In November 2000, another neutrino detector, the Sudbury Neutrino Observatory (SNO), came on line and recently in June 2001 reported their first measurements of the  $^8\text{B}$  solar neutrinos via the charged current scattering and elastic scattering on electrons, confirming oscillation of electron neutrinos to the muon- or tau-neutrinos and also ruling out models of oscillation into sterile neutrinos. Also, the SNO results currently favor the LMA solution and small mass difference between neutrinos mass eigenstates.

There have been intense efforts underway in the U.S., the Europe and the Japan for the development of an accelerator based intense neutrino source. A number of concepts exist to produce neutrino beams, all of which involve neutrino decay emissions. Currently existing neutrino beams are based on pion beams that decay in straight channels. The current beams are limited in intensities but does have physics potential as 'superbeams'. In the recent four years, muon storage ring as an intense neutrino source was most extensively studied in the U.S., Europe, and Japan. [ref\_muRing]. Beyond the traditional concepts, we mention here a recent novel

concept that utilizes short-lived radioactive nuclear particles, such as  ${}^6\text{He}$ , in a storage ring [ref\_he6ring].

The concept of a neutrino source from pion decay from a storage ring of pions was originally considered by Koshkarev in the 1960's [ref\_piRing]. However, the intensity of the muons created within the ring from pion decay was too low to provide a useful neutrino source. In 1997, the physics potential of neutrino beams produced by muon storage rings was investigated by S. Geer et al at a Fermilab workshop, where it became evident that the neutrino beams produced by muon storage rings needed for the Muon Collider were exciting on their own merit. The Neutrino Factory concept quickly captured the imagination of the particle physics community, driven in large part by the exciting atmospheric neutrino deficit results from the Super-K experiment [ref\_superK]. Recently, members of the Neutrino Factory and Muon Collider Collaboration, undertook two studies for entry level of a neutrino factory to be at either the Fermilab or the BNL, generating two important documents Study I and Study II detailing the concept, technical issues and solutions, and the costing.

In the fall of 1999, Fermilab undertook a Feasibility Study (“Study-I”) of an entry-level Neutrino Factory. One of the aims of the Study-I was to determine whether the Fermilab accelerator complex could be made to evolve into a Neutrino Factory. Study-I answered affirmatively. Simultaneously, Fermilab launched a study of the physics that might be address by such a facility. More recently, Fermilab initiated a study to compare the physics reach of a Neutrino Factory with that of conventional neutrino beams powered by a high intensity proton driver, which are referred to as “superbeams”. The aim was to compare the physics reach of superbeams with that of a realistic Neutrino Factory. It was determined that a steady and diverse stream of physics will result along this evolutionary path, i.e., that a superbeam addresses fundamental neutrino physics beyond that available using a conventional beam, and that a Neutrino Factory can go even further [ref\_SnowmassM6].

More recently, BNL organized a follow-up study (“Study-II”) on a high-performance Neutrino Factory sited at BNL. Study-II was recently completed. An important goal of Study-II was to evaluate whether BNL was a suitable site for a Neutrino Factory; that question was answered affirmatively. Figure 1 shows a comparison of the performance of the neutrino factory designs in Study I and Study II. Both Study-I and Study-II were carried out jointly with the MC, which has over 140 members from many institutions in the U.S. and abroad.

In these studies, neutrino source is to be sited at either the FNAL or the BNL pointing the beam to the underground WIPP in Carlsbad, NM. In this document, we propose to study the feasibility for siting a Far Detector of various neutrino detector types at WIPP for either neutrino factories or superbeams. Also, these detectors for neutrino detection are required to be very large in volume and can function as detectors for solar neutrinos and supernova burst neutrinos within our own Galaxy.

### 1.3 Neutrino physics

The neutrino presently holds a place in the Standard Model as a neutral, massless lepton, that comes in three families, each family associating a neutrino with a corresponding charged, massive lepton, the latter being the electron, muon, and tau particles. There are also three antineutrinos

associated with the neutrinos. There is no theoretical requirement that neutrinos have zero mass. In fact, a large number of GUT's (Grand Unified Theories) now predict non-zero mass. Experiments examining the tail of the beta decay spectrum of tritium claim to have established an upper limit of 3-5 eV for the electron neutrino mass. A massless neutrino will react only through the weak interaction, and as a result neutrinos have a very small cross-section in collisions with other particles. A neutrino particle of energy in the MeV range will traverse in lead with an average pathlength of a few lightyears before it scatters.

In 1968 Pontecorvo [ref\_Pontecorvo] showed that if neutrinos do have mass, then neutrino oscillations from one flavor to another should occur if neutrino mass eigenstates do not correspond to the weak interaction eigenstates, i.e., there is neutrino flavor mixing. Numerous experiments to detect neutrino oscillations have since been carried out. These oscillation experiments have the disadvantage of not directly measuring the neutrino masses, but only the difference in mass between neutrino mass eigenstates. The neutrino oscillations predicted by Pontecorvo are called vacuum oscillations, which occur without the benefit of reactions with normal matter. Oscillations due to matter effects were later predicted by Wolfenstein [ref\_MSW] and Mikheyev and Smirnov [ref\_MSW], collectively known as the MSW effect. Both effects are functions of the mass differences between the three neutrino mass eigenstates. Based upon the results of experiments, it is normal to assume a mass hierarchy which greatly simplifies the calculations used for predicting oscillations. Of the two independent mass differences between the three neutrinos, one mass difference is assumed much greater than the other mass difference. Where  $\underline{\Delta}m_{ji}^2 = m_j^2 - m_i^2$ , it is assumed that  $\Delta m_{32}^2 > \Delta m_{31}^2 > \Delta m_{21}^2$ . Here the  $ij$  are assigned the numbers 1, 2, and 3 which represent the three neutrino flavors of  $e, \mu$ , and  $\tau$  respectively. We also assume that the three  $\Delta m_{ji}^2$  are positive, but this is yet to be determined by experiment.

### 1.3.1 Vacuum oscillations

The time evolution of a flavor eigenstate of neutrinos propagating through vacuum is given by

$$i \frac{dV_\alpha}{dt} = U_{\alpha j}^* e^{-iE_j t} v_j, \quad (1)$$

where  $E_j$  is the neutrino energy and  $U_{\alpha j}$  is the mixing matrix connecting the flavor eigenstates  $\alpha$  with the mass eigenstates  $j$ .

$$v_\alpha = U_{\alpha j} v_j. \quad (2)$$

With three neutrinos, the mixing matrix  $U_{\alpha j}$  is the 3x3 unitary Maki-Nagawa-Sakata matrix [ref\_MNS],

$$\begin{pmatrix} c_{13}c_{12} & c_{13}s_{12} & s_{13}e^{-i\delta} \\ -c_{23}s_{12} - s_{13}s_{23}c_{12}e^{i\delta} & c_{23}c_{12} - s_{13}s_{23}s_{12}e^{i\delta} & c_{13}s_{23} \\ s_{23}s_{12} - s_{13}c_{23}c_{12}e^{i\delta} & -s_{23}c_{12} - s_{13}c_{23}s_{12}e^{i\delta} & c_{13}c_{23} \end{pmatrix}. \quad (3)$$

The  $c_{jk}$  are  $\cos\theta_{jk}$  and the  $s_{jk}$  are  $\sin\theta_{jk}$ , with  $\theta_{jk}$  being the mixing angle between neutrino mass

eigenstates  $j$  and  $k$ . The probabilities derived in this manner for a three flavor-mixing scenario are complicated expressions of the  $\Delta m_{jk}^2$  and  $\theta_{jk}$  similar to

$$P(\nu_e \rightarrow \nu_\mu) = k_{32} \sin^2 \Delta_{32} + k_{31} \sin^2 \Delta_{31} + k_{21} \sin^2 \Delta_{21} + J, \quad (4)$$

with  $\Delta_{jk} \equiv \frac{\Delta_{jk}^2 L}{4E_\nu} = 1.27 \left( \Delta m_{jk}^2 \frac{L}{E_\nu} \right)$ ,  $\Delta m_{jk}^2$  in  $\text{eV}^2$ ,  $L$  in km, and  $E_\nu$  in GeV.

The  $k_{jk}$  are complicated constant functions of the  $\theta_{jk}$  and  $\delta$ , and the last term  $J$  is a CP violation function discussed in § 1.3.3. By making the assumptions that the source-detector distance will be near the leading oscillation maximum, and that the effect reported by the LSND experiment (§2.1) is not valid, and using the present best values of the neutrino parameters, these complicated relations can be reduced into much more simplified ones.

Here  $L$ , the baseline length of the experiment, has replaced the oscillation time by assuming the neutrino velocity the same as the velocity of light  $c$ .  $L$  is expressed in km and  $E_\nu$  is in GeV.

**Error!**

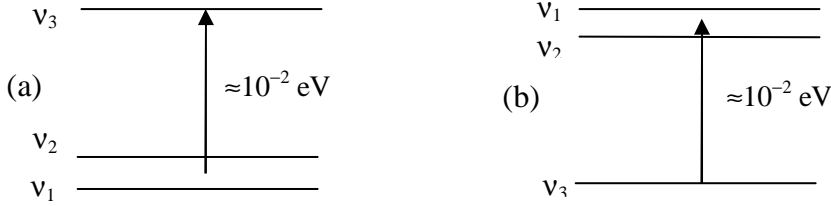


**Figure 1.** Schematic neutrino mass of (a) normal hierarchical and (b) inverted hierarchical spectra.

In the case of neutrino mass hierarchy with the lower two states having almost the same values, i.e.  $\Delta m_{21}^2 = \Delta m_{sol}^2 \ll \Delta m_{31}^2 \approx \Delta m_{32}^2 = \Delta m_{atm}^2$ , probabilities of the transition between weak eigenstates can be written as,

$$P(\nu_\mu \rightarrow \nu_\tau) = \sin^2(2\theta_{23}) \cos^4(\theta_{13}) \sin^2 \left( \frac{\Delta m_{atm}^2 L}{4E_\nu} \right),$$

$$P(\nu_e \rightarrow \nu_\mu) = \sin^2(2\theta_{13}) \sin^2(\theta_{23}) \sin^2 \left( \frac{\Delta m_{atm}^2 L}{4E_\nu} \right), \quad (5)$$

$$P(\nu_e \rightarrow \nu_\tau) = \sin^2(2\theta_{13}) \cos^2(\theta_{23}) \sin^2 \left( \frac{\Delta m_{atm}^2 L}{4E_\nu} \right),$$

where  $L$  is the baseline length and  $E_\nu$  is the energy of the neutrino beam.

### 1.3.2 Matter oscillations

When neutrinos pass through normal matter, electron neutrinos can forward scatter off the electrons in the matter. This scattering may be either neutral current (NC) or charged current

(CC) scattering. The NC scattering will affect the three neutrino flavors equally, while the CC scattering will only affect the electron neutrinos, there being only electrons (no muons or taus) in the matter traversed. By ignoring the NC scattering and assuming no CP violation, the evolution equation in the flavor basis then becomes [ref\_MSW]

$$i \frac{dv_\alpha}{dt} = \left( U_{\alpha j} \frac{m_j^2}{2E_\nu} U_{jk}^* + \delta_{\alpha k} \frac{A}{2E_\nu} \right) v_k, \quad (6)$$

where  $A/2E_\nu$  is the potential of the forward charge current scattering between  $\nu_e$  and  $e^-$  and  $A$  is defined as  $A \equiv 2\sqrt{2}G_F N_e E_\nu = 7.6 \times 10^{-5} Y_e \rho E_\nu$  with  $G_F$  as the Fermi constant,  $N_e$  the electron density,  $Y_e$  the electron fraction, and  $\rho$  the matter density. The effect is analogous to the effect on photons from the refractive index of a material as the photon travels through the material. Since there are no muons or taus present in normal matter, muon or tau neutrinos will not experience the same effect, and phase velocity differences will be established between electron neutrinos and muon or tau neutrinos. The result will be flavor oscillations. If we define a variable  $B$  as

$$B \equiv \left( \cos 2\theta_{13} - \frac{A}{\Delta m_{32}^2} \right)^2 + \sin^2 2\theta_{13}, \quad (8)$$

the oscillation probability equations will remain similar to the vacuum case, except that the vacuum mixing angle  $\theta_{13}$  and the oscillation length in vacuum ( $l = 4\pi E_\nu / \Delta m_{32}^2$ ) becomes  $\theta_{13}^m$  and  $l^m$  in matter, with

$$\sin^2 2\theta_{13}^m = \frac{\sin^2 2\theta_{13}}{B}$$

and

$$l^m = \frac{2.48 E_\nu}{\Delta m_{32}^2 B} = \frac{l}{B}. \quad (9)$$

The probability of oscillations can then be simplified by assuming the mass hierarchy and that path lengths are near the oscillation maximum.

$$P(\nu_\alpha \rightarrow \nu_\beta) = \frac{\sin^2 2\theta_{31}}{B} \sin^2 \left( \sqrt{B} \frac{1.27 \Delta m_{32}^2 L}{E_\nu} \right). \quad (10)$$

It can be seen from equations (8-10) that the maximum of matter caused oscillations will occur at a resonance point where

$$\frac{\Delta m_{32}^2}{2E_\nu} \cos 2\theta_{13}^m = A. \quad (11)$$

If the neutrinos are antineutrinos, then the value of  $A$  will be negative ( $Y_e - Y_{\bar{e}}$ ), and the oscillations will be greatly reduced. Taking the cosine factor as positive,  $\Delta m_{32}^2$  would have to be negative in order to have similar oscillation amplitudes for neutrinos as antineutrinos at the same parametric values. This should provide good experimental discrimination between positive and

negative  $\Delta m_{32}^2$ .

Neutrino flight paths that remain entirely within the Earth's crust from source to detector (distances less than 3,000 km) will have a relatively constant density, and calculations can be made with  $\rho = \text{constant}$ . For baseline experiments longer than 3000 km, the paths would take the neutrinos through the Earth's core and upper mantle, thereby subjecting them to variable density. Calculations for these trajectories need to be integrated over the whole flight path.

### 1.3.3 CP violation

Oscillation probabilities for neutrinos and antineutrinos will differ if CP is not conserved, providing a potential method for detecting CP violation. With only one phase angle  $\delta$  in the mixing matrix, there should only be one CP-odd oscillation asymmetry. CP essentially acts as the particle-antiparticle conjugation. Therefore, if CP is conserved,

$$P(\nu_\alpha \rightarrow \nu_\beta; t) = P(\bar{\nu}_\alpha \rightarrow \bar{\nu}_\beta; t) \quad (12)$$

Defining  $\Delta P_{\alpha\beta} \equiv P(\nu_\alpha \rightarrow \nu_\beta; t) - P(\bar{\nu}_\alpha \rightarrow \bar{\nu}_\beta; t)$  as the CP-odd asymmetry,

$$\Delta P_{e\mu} = \Delta P_{\mu\tau} = \Delta P_{\tau e} = 4J \left[ \sin\left(\frac{\Delta m_{21}^2}{2E} t\right) + \sin\left(\frac{\Delta m_{32}^2}{2E} t\right) + \sin\left(\frac{\Delta m_{31}^2}{2E} t\right) \right] \quad (13)$$

where  $J = s_{12}c_{12}s_{13}c_{13}^2s_{23}c_{23} \sin \delta$

is the Jarlskog factor and the  $J$  used in equation (4). If any of the mixing angles are zero or  $90^\circ$ , or if any of the  $\Delta m_{ji}^2$  are zero, then the asymmetry will disappear. Even if this is not the case, it can be seen that small mixing angles will likely keep the effect small. In the case of very large oscillation phases, averaging of the *sine* terms causes the effect to approach zero [ref\_CP]. For these reasons it is probable that any hope to detect CP violation through oscillation studies must be done at shorter baselines where matter effects will not obscure CP results.

## 1.4 Neutrino Physics from Galactic Supernova Burst

The historical supernova record for the past 2000 years applies to the local 4-5 kpc of the Galaxy, beyond which the supernovae are not optically visible. From the spiral arm structure shown by radio maps of the Galaxy, it appears that this local sample is representative, covering portions of three spiral arms, and contains about 8% of the disc stars. The number recorded in 2000 years extrapolates to the whole Galaxy to give an expected rate of about  $6 \pm 1$  / century. This is about a factor two higher than the rate  $3 \pm 1$  / century estimated by other astrophysical methods (e.g. expected stellar death rate) the difference being statistically significant at the 95% confidence level. Whether the interval is 15-20 years, or 30-40 years, there is increasing support for the view that large detectors should run continuously with the aim of obtaining the unique neutrino data which supernova burst would provide.

A supernova releases  $> 99\%$  of its energy in the form of neutrinos, divided approximately equally between the three neutrino types and their anti-particles. However, the muon- and the tau- neutrinos/anti-neutrinos (11 MeV/16MeV). The energy dependence and thresholds of the neutral current cross section results in the nuclear excitation process strongly favoring the muon- and tau- neutrino component of the burst. Thus, detection based on excitation of Pb and Fe nuclei would provide a signal complementary to that of other world detectors sensitive principally to electron anti-neutrinos. The time profile of the muon- and tau- neutrino burst would be distorted by non-zero masses down to about 10 eV, or down to 3 eV in the case of black hole formation [ref\_SNBeacom].

Mixing effects, either vacuum or MSW in the supernova, result in departures from the approximately equal numbers of different neutrino types arriving at the Earth. An important additional effect is the conversion of muon- and tau- neutrinos to e- neutrinos of correspondingly high momentum, and these would produce a sharp increase in charged current nuclear excitation, observable in the Pb target by the production of a population of two-neutron events [ref\_FHM] which, in an optimized design, can be efficiently and accurately counted [ref\_Smith] in addition to the single neutron events. The supernova burst can provide a much wider MSW range of  $\sin^2 2\theta$  (down to  $10^{-8}$ ) and  $\Delta m^2 = 10^{-19} \text{ eV}^2$  due to the very long path length (typically 4 – 20 kpc).

We can summarize the neutrino physics goals from this higher-flavor neutrino signal, in association with the e anti-neutrino signal from other world detectors as follows:

- (a) Direct mass limits that can confirm the recent SNO results. Currently, the LMA solution supported by the SNO results puts the mass limit at 2 eV for the  $\tau$  neutrino [ref\_SNO].
- (b) Black hole formation would cause abrupt termination of neutrino luminosity, with the  $\nu_e$  signal terminating  $\sim 100 \mu\text{sec}$  earlier than the  $\nu_\mu$  and  $\nu_\tau$  signal. The proposed scheme would allow this precision measurement in the time profile, and in addition to providing a clear indication of black hole formation, the sharpness of the cut-off would allow neutrino mass measurement (or limits) to be extended down to the region 2-3 eV [ref\_SNBeacom].
- (c) If all neutrino masses lie in the sub-eV range, then the time profiles will still provide new information on neutrino mixing. Mixing of  $\nu_{\mu,\tau}$  to  $\nu_e$  will produce high momentum  $\nu_e$  enhancing the charged current signal. This significantly increases total neutron production for both Pb and Fe targets, but in addition produces a remarkable factor  $\sim 60$  increase in two-neutron events in Pb. Since the latter effect will occur in Pb but not in Fe, this indicates the importance of using both Fe and Pb targets.
- (d) Mixing to sterile neutrinos would result in loss of one flavor, and hence, unequal numbers of different flavors. This would be revealed by comparison with signals from  $\nu_e$  detectors. This process may also give rise to different time profiles (in addition to different total events) for one-neutron and two-neutron signals in the Pb and the Fe detectors. SNO results currently rules out complete oscillation into sterile neutrinos.
- (e) Other processes within the supernova – in particular hydrostatic vibrations and details of the neutronization process for  $\nu_e$ , could also be inferred from the neutrino time profiles.



Instrumenting the Far Detector for the supernova burst would add three new time profiles dominated by  $\nu_{\mu,\tau}$  (single neutron from Fe, single-neutron and double-neutron from Pb) to the two time profiles provided by existing detectors ( $\bar{\nu}_e$  charged current from Super-K and SNO, neutral current from both Super-K and SNO), making a world total of five different time profiles containing 10,000-15,000 events which would provide a wealth of new information both on neutrino physics and on details of the supernova mechanism.

- (f) Neither production in the supernova nor neutral current detection distinguishes between  $\mu$  and  $\tau$  neutrinos. Thus, mixing via  $\theta_{12}$  and  $\theta_{13}$  can be deduced without any effects arising from  $\theta_{23}$ . Measurement of excitation cross sections in Pb using for example the proposed ORLAND facility, will enable the mixing signal to be calibrated sufficiently to allow numerical estimates to be made of both  $\theta_{12}$  and  $\theta_{13}$ , together with the corresponding values of  $\Delta m^2$ .
- (g) The MSW effect applies only to neutrinos (not anti-neutrinos). MSW oscillations will therefore affect the  $\mu$  and  $\tau$  neutrino flux measured in the Pb and Fe targets (since these neutrinos are pair produced in the supernova) and the directional  $e$  neutrino signal in Super-K, but not the dominant  $\bar{\nu}_e$  signal in Super-K.
- (h) The ratio of two-neutron to one-neutron events will measure the electron-neutrino fraction in the higher-momentum region of the supernova neutrino spectrum. This can be compared with the electron anti-neutrino spectrum and time profile measured by Super-K. The various oscillation scenarios from solar and atmospheric neutrino oscillation experiments then give the following signatures:
  - 1) In large angle MSW mixing of  $\nu_e$  to  $\nu_{\mu,\tau}$ , such as the LMA and LOW solutions to the solar neutrino problem, the survival probability of  $e$  neutrinos (in a two-flavor model) is basically given by the electron neutrino content of the heavy mass eigenstate. The Far detector signal will see the inverse of this, i.e. it measures the electron neutrino content of the light mass eigenstate. With a large mixing angle, the vacuum oscillation of anti-neutrinos may also be significant, which will reduce the  $\nu_e$  flux measured at Super-K.
  - 2) In small angle mixing, the conversion is essentially complete if the mixing parameters lie with the triangular area on the standard plot. The SMA solution to the solar neutrino problem lies close to the edge of this triangle, whose slope depends on the assumed form of the density distribution in the supernova, and a more detailed calculation is required to give exact predictions.
  - 3) For the “just-so” vacuum oscillation solution to the solar neutrino problem, the much longer baseline to the supernova would result in complete mixing of both neutrinos and anti-neutrinos, yielding a two-neutron signal similar to that tabulated in the proposal. This can be distinguished from MSW mixing by the fact that Super-K would see a radically reduced  $\bar{\nu}_e$  signal.

Further effects on the neutrino time profiles, such as the flavor of the initial neutronization spike, the question of inverted or normal mass hierarchy, and earth matter effects, have been studied by Dighe and Smirnov, and shown to be observable in principle [ref\_SNDighe].

Some of the above physics can be deduced with only a few hundred events, but others in particular, the simultaneous measurement  $\theta_{12}$  and  $\theta_{13}$ , will require several thousand events from both the Pb and Fe targets. We will now show that the Far Detector could provide numbers of this order from an 8 kpc supernova.

## 2 NEUTRINO EXPERIMENTS

### 2.1 Past experiments

Impetus for the direct detection and measurement of the mass of neutrinos in the past has come mainly from astrophysics. Solar models had been developed which were capable of predicting the solar neutrino flux, and cosmic ray measurements and simulations had predict atmospheric neutrino fluxes. When experiments were performed which did not agree with these predictions, a new level of interest in neutrino experiments was created.

The first experiment to detect the solar neutrino flux was carried out at Homestake Gold Mine in South Dakota in 1957 by R. Davis [ref\_RayDavis]. The neutrino target was 615 tons of tetrachloroethylene located underground, and the detection was of Auger electrons produced by electron capture in  $^{37}\text{Ar}$ , itself produced by electron neutrino interaction with the  $^{37}\text{Cl}$  in the  $\text{C}_2\text{Cl}_4$ . The  $^{37}\text{Ar}$  was periodically swept from the tank for analysis. Standard solar model (SSM) predictions of 4.1 to 9.3 solar neutrino units for  $^{37}\text{Cl}$  (SNU) by different investigators were all higher than the average of 2.56 SNU detected at Homestake after 108 runs. The results were later confirmed by Kamiokande, GALLEX, and SAGE, which led to the present state of the solar neutrino puzzle.

The most important experiment for the detection of solar and atmospheric neutrinos has been the Super-Kamiokande experiment (1996), with a large target mass and high statistical significance. This detector used water as the neutrino target and PMT's as the detectors. Cherenkov light produced from neutrino-electron scattering within the water is detected. The fiducial mass of the target was 22,500 tons. This detector was sensitive to  $^8\text{B}$  solar neutrinos, and reported a deficit in these neutrinos as compared to the SSM predictions. The experiment also reported detecting oscillations of atmospheric neutrinos evidenced by the disappearance of upward-going muon neutrinos. Super-K reported that the muon neutrinos were not going to electron neutrinos, but being unable to detect taus, was unable to determine whether the muon neutrinos were going to tau neutrinos or sterile neutrinos. Super-K has recently reported that oscillations to sterile neutrinos is disfavored. MACRO has also report a deficit of atmospheric muon neutrinos from below, with no deficit from above. The deficit and angular distributions were interpreted in terms of neutrino oscillations.

There have been several experiments for detecting neutrinos originating from both nuclear reactors and particle accelerators. Chooz and Palo Verde were detectors 1 km distant from nuclear reactors, both using gadolinium (Gd) loaded liquid scintillators. Although showing no evidence of oscillation, they were able to place limits on the oscillation parameter spaces.

LSND and Karmen were accelerator experiments. In the LSND experiment a mixed neutrino beam was created from the decay of pions, which had been produced when 800 MeV protons struck a beamstop. The target was 52,000 gallons of mineral oil augmented with a liquid scintillator. The detectors of Cherenkov and scintillation light were 1220 PMT's. This experiment reported the detection of muon neutrino to electron neutrino oscillations within a range of neutrino parameters excluded by atmospheric and solar experiments in a three neutrino theory. KARMEN2, an upgraded KARMEN, utilized a beam stop neutrino source and 56 metric tons of liquid scintillator, but without detecting an oscillation signal.

The LSND experiment was the only one of the reactor or accelerator experiments to show evidence for neutrino oscillations. The evidence was the appearance of electron neutrinos from a beam of muon neutrinos, and provided an allowed oscillation area in the parameter space of  $\Delta m_{ij}^2$  and  $\sin^2(2\theta_{ij})$ , the latter being the mixing angle between flavors. Other reactor/accelerator experiments found no oscillations, but did provide exclusion areas in the parameter space. If positive results for neutrino oscillations from atmospheric and solar neutrino experiments are combined with the LSND results, a third, independent  $\Delta m_{ij}^2$  is required in the mass hierarchy. For three independent  $\Delta m_{ij}^2$ , four neutrinos are required. The fourth neutrino is beyond the standard model, and would be a sterile (no weak reactions) neutrino. The LSND experiment has not been confirmed by any other experiment, but efforts are underway to do so.

The CHORUS [ref\_CHORUS] detector operated in conjunction with the CERN SPS Wide-Band Neutrino Beam. It is designed primarily to detect  $\nu_\mu \rightarrow \nu_\tau$  oscillations. The detector was a near detector using both 770 kg of nuclear emulsions and an electronic fiber tracker with an air-core magnet. In data taken from 1994 through 1997, no  $\nu_\mu \rightarrow \nu_\tau$  oscillations were detected [ref\_CHOSUS]. Exclusion areas of the parameter space were established.

Solar and atmospheric neutrino experiments like Super-K and LSND, by studying neutrino oscillations, have narrowed the range of the neutrino parameter spaces,  $\Delta m_{ij}^2$  and  $\sin^2\theta_{ij}$ . The various explanations given of present experimental results postulate both vacuum and matter oscillations, as well as sterile neutrinos. The principal explanations are the large angle MSW, small angle MSW, LOW MSW, and mixed atmospheric, solar, and LSND. Much work remains to be done in order to arrive at a satisfactory theoretical basis upon which all experiments can agree, and then to define and measure all of the lepton sector parameters accurately.

## 2.2 Present experiments

Experiments like Super-Kamiokande and KARMEN2 continue to operate in an effort to improve their statistics with additional running time. Some of these experiments have been enhanced with beams or new detectors to make them more effective.

K2K (KEK to Kamioka), a baseline experiment of 235 km from KEK to Super-K in Japan, is searching for  $\nu_\mu$  disappearance and is presently taking data. There is a near detector, consisting of a 1 kton water Cherenkov detector, a scintillating fiber tracker, a muon ranger, and an electromagnetic calorimeter. The near detector is used for normalizing the beam flux. The far detector is the Super-K water Cherenkov detector. This experiment should be able to explore all but

the smallest  $\Delta m_{ji}^2$  region of the parameter space allowed by Super-K. The first detection of neutrinos from KEK were in June, 1999.

A real-time solar neutrino experiment is operating at Sudbury Neutrino Observatory (SNO) in Ontario, Canada, that is sensitive to both weak neutral and charged currents. This detector consists of 1000 ton of deuterium, with highly purified NaCl added to capture freed neutrons in the NC reactions of all neutrinos with deuterium, emitting 8 MeV gammas. The thousands of PMT's will be able to separately identify the CC reactions of electron neutrinos above about 5 MeV. This makes it possible to separate solar electron neutrinos from total solar neutrinos. The detector began observing solar neutrinos in 2000. Preliminary results in 2001 (before the addition of NaCl) indicate that about 2/3 of the energetic electron neutrinos have oscillated into muon and tau neutrinos, while the total number of neutrinos is in good agreement with the SSM.

### 2.3 Future experiments

A longer baseline experiment, approximately 730 km, is in development. MINOS, located in the Soudan mine in Minnesota, will operate with a neutrino beam from Fermilab, and will be capable of studying NC/CC energy distributions. MINOS will have both a near detector, located just downstream of the pion decay channel, and a far detector located at Soudan. Both detectors are similarly constructed, consisting of layers of scintillation detectors sandwiched between thin iron plates. Large electromagnets will provide a toroidal magnetic field within the steel plates. The near detector will have a 0.1 metric kt fiducial mass, and the far detector will have a 3.3 metric kton fiducial mass. MINOS is scheduled to begin taking data in 2002.

MiniBooNE is under construction at Fermilab in order to search for  $\nu_\mu \rightarrow \nu_e$  oscillations as a check on the LSND experiment. Neutrinos from pion decay produced by 8 GeV protons on a beryllium target will be sent to a detector located 490 m from the end of the decay channel. The detector consists of 800 tons of scintillating mineral oil in a large spherical tank, augmented with 1280 photo-detectors covering a 445 ton fiducial volume. Mini-BooNE is scheduled to begin taking data in 2002.

ICARUS-II is an ambitious program, highlighted by a new liquid argon time proportional chamber (TPC), to be located at Gran Sasso, Italy. The first phase is a 600 metric ton TPC. This module will be capable of detecting atmospheric and solar neutrinos. With the addition of more modules to carry the mass to 5000 tons and a neutrino beam from CERN CNGS, ICARUS should be well situated to carry on advanced studies of neutrino oscillations. ICARUS should be capable of detecting tau appearance, with implications for the sterile neutrino theory. Data from the first 600 ton is shown in fig. 1.

OPERA is a proposed experiment to utilize the same CNGS beam as ICARUS. The difference is that the proposed OPERA detector is a nuclear emulsion detector, utilizing real-time automatic analysis of the emulsions. Being a fine grained detector, the emulsion detector will be suitable for tau appearance experiments. Since this can also be accomplished by ICARUS, OPERA may have difficulty in obtaining approval.

Although it is impossible to predict the outcome of these and perhaps other experiments planned for the next few years, it is reasonable to assume that collectively (in the absence of a

sterile neutrino) these experiments will be able to determine  $\Delta m_{ij}^2$  and  $\sin^2(2\theta_{ij})$  to a reasonable accuracy O(10%). It will probably be possible to determine if the need for a sterile neutrino actually exists. It is not so likely that much progress will be made on confirming matter oscillations, CP violation, or determining the values of  $\Delta m_{ij}^2$  and  $\sin^2(2\theta_{ij})$  to greater accuracies. New experiments will be required for this, based on longer baselines and better neutrino beams and detectors. These experiments while proposed to do studies using neutrino beams, some of them can also be adapted to run in supernova monitor mode to detect burst of neutrinos from supernova neutrino within our own galaxy.

### 3 NEUTRINO FACTORY

of which is *A Feasibility Study of a Neutrino Source Based on a Muon Storage Ring*, a study initiated at Fermilab. A parallel study entitled *Physics at a Neutrino Factory* was also prepared. The former paper considers aspects of construction of such a factory, and the later considers the variety of physics studies that could be pursued if there were such a factory. A similar study written for a muon collider, but with consideration of a neutrino factory, is presently underway at Brookhaven National Laboratory. A future neutrino factory at CERN is also serious possibility. The descriptions of a possible neutrino factory below come from the Fermilab study.

#### 3.1 Design elements

Neutrinos from a neutrino factory will be created from the decay of muons contained in a muon storage ring. The storage ring in turn will receive muons from the decay of pions and kaons created by the high energy impact of protons onto a fixed target. For a design goal of  $2 \times 10^{20}$  neutrinos produced per operational year ( $2 \times 10^7$  sec), a rate of  $4.5 \times 10^{14}$  protons per second on target at 16 GeV would be required, furnished in cycles at 15 Hz, 12 bunches per cycle, each lasting 80  $\mu$ s and containing  $2.5 \times 10^{12}$  protons. With upgrades, most of the present Fermilab facilities could be used to provide these protons. Before reaching the muon storage ring, intermediate particles have to be selected, accelerated, and cooled in numerous stages to supply  $9 \times 10^{20}$  unpolarized muons per operational year to the storage ring at energies up to 50 GeV.

The proposed storage ring would be in the shape of a racetrack  $813 \times 86$  meters, with the two end radiuses at 43 meters. The long racetrack design must be angled down into the ground in order to allow the beam to be directed at a distant target, thus only one side of the racetrack can produce usable neutrinos. The Fermilab design angles the beam down at  $13^\circ$ , but could change depending on the detector location. A production straight in one side of the racetrack represents approximately 39% of the circumference, which establishes a maximum percent utilization of the produced muons. Geological and cost considerations limit the length of the racetrack at this angle to the listed length, and thus the maximum percent utilization is also limited if the angle does not change. The average survival time of a 50 GeV muon in the storage ring is 178 turns. Other shapes have been proposed, such as a "bow tie" shape, which would allow for neutrinos to be projected in two directions [ref\_Garren].

## 3.2 Beam characteristics

The design given above results in an expected  $6 \times 10^{19}$  muon decays per year in the production straight, somewhat short of the goal of  $2 \times 10^{20}$ . The difference was ascribed to muon decays in the various subsystems. Each muon decay will result in one muon neutrino and one electron antineutrino. Should positive muons be selected for the storage ring, the decays will provide one electron neutrino and one muon antineutrino. These ratios are fixed, and other neutrino backgrounds in the beam are nonexistent. The energy range of the muons will extend from 10 GeV to 50 GeV. The characteristics of the neutrino beam at the detector are directly related to the conditions imposed upon the muons in the storage ring. The muon energy spectrum and transverse beam divergence are the most important variables and must be known accurately. Longitudinal divergence is not so important as most neutrino experiments are integrated over long running times.

### 3.2.1 Beam divergence

Neutrino beam divergence should depend upon both muon beam divergence and on muon energy in the production straight. As described in more detail below, virtually all of the neutrinos from muon decays will be focused in the extreme forward direction. This is due to the relativistic boost effect on the neutrinos from the high energy of the muons, commonly known as the "headlight effect". Divergence due to the decay kinematics of the muon is therefore a function of muon energy, and the neutrino spread angle is basically  $1/\gamma$ . The neutrino factory design includes the specification that the transverse emittance of the muon beam must be less than 10% of the kinematic mean decay angle, the latter being only 2 mr at 50 GeV. With this specification in force, the total neutrino beam divergence will only be a function of the beam energy.

### 3.2.2 Beam flux at the target

The relativistic "headlight effect" on the neutrino beam at the target can be calculated to give either the neutrino flux or the percentage of all neutrinos produced that arrive in a selected area of the target. The flux works out to be

where  $n_0$  is the number of neutrinos per unit time from decayed muons,  $L$  is the length from factory to target,  $\gamma_\mu = E_\mu/m_\mu$ ,  $\beta_\mu = p_\mu/E_\mu$ , and  $\theta$  is the angle between the beam axis and a point on the target. For long  $L$  the angle  $\theta$  is very small and  $\cos \theta$  can be approximated by 1. Using the series approximation  $\beta_\mu = 1 - 1/2\gamma_\mu^2$ , the neutrino flux may be approximated by

At  $L$  of 1000 km and energies of 50 GeV, the flux intensity will remain essentially constant out to a distance of 1 km from the axis of the beam. Thus a detector located within a cone with vertex angle of 2 mr should always be located within a flat, high flux portion of the beam.

### 3.2.3 Beam spectra

The energy distribution of muon neutrinos (antineutrinos) from the decay of non-polarized muons and anti-muons is given in the muon rest-frame by the following proportionality.

For electron neutrinos (antineutrinos) the relation is

where  $x = 2E_{\nu} / m_{\mu}$  is a scaling variable and  $\theta$  is the angle between the muon spin and neutrino momentum vectors. The term with  $\cos\theta$  will disappear when averaged over the states of the initial muons. In the laboratory frame where  $m_{\mu} \rightarrow \gamma m_{\mu}$ ,  $E_{\mu} \rightarrow \gamma E_{\mu}$ , and  $x \rightarrow \gamma E_{\nu} / E_{\mu}$ , equations (19) and (20) will allow the calculation of beam spectra as a function of muon energy. The total decay rate expressions are not required since all muons will ultimately decay in the storage ring.

The results of the spectrum calculations show that neutrino energies will encompass the whole spectrum up to the muon energies. For neutrinos the spectral intensity peaks at the muon energy, while for antineutrinos the spectral intensity peaks at approximately 65% of the muon energies, and then tails off to zero. The mean neutrino energy is about 73% of the muon energy while the mean antineutrino energy is about 61% of the muon energy.

The muon accelerator introduces muons to the storage ring with energies to 50 GeV and a  $\Delta E_{\mu} / E_{\mu} < \pm 2\%$ . The Fermilab report does not specify if the storage ring modifies this dispersion, but assuming no changes are brought about by the storage ring, then  $\Delta x_{\mu} / x_{\mu} < \pm 2\%$ . This will cause a slight spreading in the neutrino spectrum of muon decay.

## 4 CONCEPTS for NEUTRINO DETECTORS

Neutrino factory beams will potentially allow all of the oscillations  $\nu_e \rightarrow \nu_{\mu}$ ,  $\nu_e \rightarrow \nu_{\tau}$ , and  $\nu_{\mu} \rightarrow \nu_{\tau}$  and their antineutrino analogs to be studied by analyzing the products of neutrino-target collisions. The success of this endeavor will depend on how many collision events of each neutrino flavor can be detected, and how well these events can be characterized and measured, all in a reasonable experimental time. The number of events detected will depend upon the cross-sections of the reactions, the mass of the detector, the flux of each neutrino type in the beam, and the characteristics of the detector. The neutrino flux composition will be modified at the detector by any oscillations which occur during the travel time to the detector. These probabilities are given in equations (5), with the reverse oscillations having the same probabilities. Antineutrino oscillation also will have the same probabilities as neutrino oscillations if CP invariance holds. In order to design an appropriate detector that will compliment the neutrino factory as described, it is necessary to understand all of the possible neutrino interactions with the target, the interaction cross sections, the interaction products, and how the products can best be detected and measured.

## 4.1 Neutrino reactions and cross sections

Neutrino interactions can be categorized as either charged current (CC) or neutral current (NC) and as acting upon either the electrons or nucleons in the target. The CC reactions are mediated by the  $W^\pm$  vector bosons which carry charge, energy, and momentum from one interaction vertex to the other, allowing for the changing of one type of particle into another. The NC reactions, mediated by the  $Z^0$  boson, do not carry charge and cannot directly change particles. NC reactions are limited to the exchange of energy and momentum between particles. The vector boson particles are massive with  $m_{W^\pm} = 83 \text{ GeV}/c^2$  and  $m_Z = 90 \text{ GeV}/c^2$ . This large mass accounts for weak reactions being short in range and weak in strength.

Reactions may be elastic or inelastic. Inelastic reactions are those in which the initial and final state particles are different. In certain cases with higher energy ranges, elastic reactions can appear to create entirely new particle. However, these particles are actually the result of momentum and energy exchanges which result in recoil or fragmentation of existing particles. The characterization of reactions by this method sometimes results in names which are more or less descriptive, but not entirely accurate.

### 4.1.1 Reactions with electrons in the target

The following neutrino reactions can take place with the electrons in the target:

where the \* represents an excited state and  $l = e, \mu, \tau$ . Reactions (a,b) will kick bound electrons in the target to higher energy levels, while reactions (c,d) will create free electrons. Reaction (e) will create a lepton with the same flavor as the reacting neutrino, similar to the more important nucleon CC reactions discussed later. Those electrons still bound to an atom will emit a  $\gamma$  upon returning to the ground state. Those electrons freed from their atom will cause an electron shower, releasing further electrons and  $\gamma$ 's, depending on the energy transferred in the reaction, until all particles are fully absorbed. The cross sections of these reactions are of order  $10^{-42} \text{ cm}^2/\text{GeV}$  [ref\_nuCrossn], three orders of magnitude lower than neutrino reactions with nucleons in the experimental range of interest, making these reactions less suitable for factory detector uses.

### 4.1.2 Reactions with nucleons in the target

Neutrino interactions with the target nucleons are a much more complicated process due to the complex structure of the nucleon. Cross-sections are calculated theoretically with reasonable accuracy, but good experimental data to verify the calculations at all energies is lacking. Experimental data is required both to check cross section calculations and to accurately determine functions, such as the parton distribution functions. Nucleon reactions are primarily neutrino-nucleon reactions at energies less than 2 GeV and neutrino-parton interactions above this energy level. The distinction, however, is a fine one, and both types of reactions occur in the border region. For the CC reactions the additional complication of resonance enhancement enters the



picture at about 500 MeV. The ratio of CC to NC reactions in the 1 GeV to 100 GeV range is approximately 3.0. This will be an important ratio in analysis of detector results.

#### 4.1.2.1 Neutral currents

Neutral current reactions do not create new particles during the interaction, but can excite the target nucleus to eject nucleons or fragment the nucleon with the appearance of new particles. In the lower energy regimes of equations (a) and (b) below, interactions can excite the nucleon, which then returns to the ground state with the ejection of a neutron from the nucleus. Neutrons or protons may also be ejected by recoil. Beside neutrino energy levels, the material of the target nucleus (A,Z) is very important in determining the ejection rates and energies. This effect is not only the result of changing cross sections per nucleon in the neutrino-nucleon reaction, but is the result of different branching ratios in the de-excitation process of the nucleus. Target material selection could then play a major role in detector target selection if these neutral current reactions are chosen for neutrino detection. These NC reactions will constitute a major source of background for CC events.

In the higher energy regimes of equations (c) and (d), the interactions can eject hadrons, such as pions, from the nucleus. The multiplicity of these ejected particles increases with increased neutrino energies, forming hadron showers. Subsequent decays of pions or kaons in the showers can result in secondary leptons which cause a background for primary lepton detection. Cross sections for NC reactions have been recently calculated based on parton distribution functions which compare favorably with experimental measurements. Cross sections for neutrino reactions (c) and (d) are approximately  $2.4 \times 10^{-39} \text{ cm}^2/\text{GeV}$  in the neutrino energy range from 10 to 50 GeV, with antineutrino cross section approximately one-half of neutrino cross sections.

#### 4.1.2.2 Charged currents

All of the charged current neutrino-nucleon interactions produce one charged lepton of the same flavor as the incident neutrino. The CC reactions can also create hadron showers in addition to a primary lepton. The nature of the reactions can again be correlated with particular energy ranges of the incident neutrinos. For energies up to 1 GeV the reactions are dominated by quasi-elastic (inelastic) scattering (QES) on the nucleon. Above 10 GeV the dominant mode is deep inelastic scattering (DIS) off of the partons in the nucleon, and in the interim energy range both types of scattering occur. Beginning at about 300 MeV, a resonance induced (RIS) inelastic scattering becomes important. The charged current reactions will be the most important of all neutrino interactions for the factory detector.

In quasi-elastic scattering (a,b) the neutrino scatters off the entire nucleon, changing a neutron to a proton for incident neutrinos, and vice versa for antineutrinos. The cross section for the reaction has been measured experimentally and compares favorably with calculated cross sections. After a threshold energy near 100 MeV is reached, the cross section rises rapidly to

approximately  $1.1 \times 10^{-38} \text{ cm}^2$  at 1 GeV, where it begins to trail off slowly. As with NC reactions, the material of the nucleus is expected to have important effects on any particles ejected.

Resonance induced scattering (c,d) can be considered one aspect of deep inelastic scattering. When the proper energy is available for the nucleon to excite to a baryon resonance, the cross section is greatly enhanced. At low energies the  $\Delta(1232)$  resonance dominates causing single pion production. As energies increase, multiplicity of pion production increases. Since there are many such resonances, calculation of the cross sections becomes quite involved. Even experimental measurements show "spike-like" behavior with large experimental errors. Resonance behavior begins at about 300 MeV and rises rapidly until 10 GeV, where it begins to level off. The cross section at 10 GeV is approximately  $1.2 \times 10^{-38} \text{ cm}^2$ . Antineutrino cross sections are slightly lower than neutrino cross sections for this mechanism.

At energies of roughly 1 GeV, deep inelastic scattering begins in which neutrinos scatter off partons in the nucleon. Cross sections for electron and muon neutrinos have been measured and calculated. The cross sections for  $\nu_\mu$  and  $\nu_e$  rise linearly with energy from 1 GeV. At 50 GeV, the maximum energy of factory neutrinos, the cross sections have risen to a value of  $3.6 \times 10^{-37} \text{ cm}^2$ . These values include RIS reactions which represents only a small fraction of DIS cross sections. In the range above 1 GeV, calculated cross sections fit within the experimental error ranges, which are as large as  $\pm 20\%$ . For deep inelastic scattering, the cross sections of antineutrinos are approximately one-half of those for neutrinos.

The cross sections of tau neutrinos are less than those of muon and electron neutrinos. This is due to parton distribution functions which are weighted by the square of the lepton mass and are negative. These terms become important for the heavier tau lepton, and thus result in lower cross sections. The tau neutrino cross section begins at about 5 GeV due to the energy threshold of the tau mass, and rises, but not as rapidly as for muon neutrinos. A cross section of  $2.2 \times 10^{-37}$  is reached at 50 GeV. Tau neutrino cross sections have not been well measured.

## 4.2 Detection methods

It is possible to detect all of the six neutrino types through their interactions with the detector target materials; however, the same methods cannot be used to detect them all. The reaction products, which are the detected particles, vary significantly for the different neutrinos. The types of reaction products to be seen are leptons, baryons, hadrons of various types, and gammas. Many of the primary product particles will decay with their passage through the detector. The taus will decay to muons, electrons, and hadrons; muons will decay to electrons; kaons will decay to muons, electrons, and pions; and pions will decay almost entirely to muons. Undetectable neutrinos will also be produced. Primary and secondary particles (excepting neutrinos) with sufficient energy can also undergo CC and NC interactions with the materials in the target and detector.

Identification of reacting neutrinos is made possible by identifying the primary lepton in CC reactions or measuring momenta and energies of hadron showers in NC or CC reactions. The differences in reactions and decays for the different neutrino flavors allows for their identification, but similarities in reactions and reaction products makes identification more difficult. To make positive identifications, it is a great advantage to be able to see a product particle's track in the detector, preferably with high resolution. It is also possible to make other measurements which help to identify a particle as well as its parent. Among these are measurement of momentum, energy, and charge of the particle. There will frequently be "unseen" energy and momentum carried away by secondary neutrinos. This energy loss must be inferred from other energy measurements.

Through all the confusion of identification, prescribed steps can be followed which organize the search more optimally. These are enumerated for a single reaction and for use when they are possible or useful:

- a) Locate the vertex of the initial reaction,
- b) Follow the track of the primary lepton to its decay, absorption, or exit from the detector,
- c) Determine the sign of the primary or daughter lepton,
- d) Follow the cascade of lepton charged particles from the primary or secondary lepton vertex,
- e) Measure the energy loss in the lepton cascade up to final absorption,
- f) Measure the momentum of the primary or daughter lepton,
- g) Follow hadron tracks from the primary vertex,
- h) Follow hadron tracks from the lepton decay vertex,
- i) Measure total energy loss in the hadron tracks,
- j) Measure transverse energy loss in the hadron tracks,
- k) Measure transverse momentum in the hadron tracks.

Studying how each flavor of neutrino and its product particles act in the detector will determine which of the above techniques will be beneficial. Ultimately, these techniques will be the determining factors in choosing a detector type, design, and particle analysis procedure.

#### 4.2.1 Tau neutrinos

The tau neutrino interaction will lead to either a  $\tau$ -lepton or to a hadron shower, depending upon whether the interaction is CC or NC. Hadrons may also occur in addition to the lepton in CC reactions. The CC/NC ratio is approximately 3.0, and thus 75% of the interactions of  $\nu_\tau$  should lead to  $\tau$ -leptons. The hadron shower from the  $\nu_\tau$  NC reaction cannot be directly distinguished from  $\nu_\mu$  and  $\nu_e$  caused showers. This makes the NC interaction unsuitable for direct identification of the  $\nu_\tau$ , although other useful means may be employed, such as determining overall NC/CC ratios.

In charged current reactions the  $\tau$ -lepton has a very short lifetime before decaying, about  $2.9 \times 10^{-13}$  sec in its rest frame. At a  $\tau$  energy representative of factory neutrino reactions, this time will increase to approximately  $3 \times 10^{-12}$  sec, or a distance travelled of less than 1 mm. The  $\tau$  will decay in one of two ways; (1) into a single charged  $\mu$ ,  $e$ , or hadron track with a distinctive

"kink" in the trajectory at the decay vertex (the lost momentum carried away by neutrinos) on the order of 100  $\mu\text{m}$ , or (2) three, five, etc. charged hadron jets depending upon energy. These are generally referred to as one, three, or five-prong reactions. The branching ratios result in 85.5% of the decays being one-prong and 14.5% being three-prong. Of the one-pronged decays, 43% have lepton products and 57% have hadron products. Five percent of the lepton decays have an additional gamma.

#### **4.2.2 Muon neutrinos**

Muon neutrino interactions will produce a primary muon (and possible hadronic material) in CC interactions and hadronic showers in NC interactions. The CC/NC ratio is again approximately 3.0. The lifetime of the primary muon produced is much longer than the tau lifetime. The muon lifetime at rest is  $2.2 \times 10^{-6}$  sec and its sole source of decay is to an electron. Many muons created in the detector will end up exiting the detector before they decay. Where the muons decay will be very much dependent upon the muon energy. Similarly muons created in the atmosphere by cosmic rays will reach the detector even when it is located underground, although the greater the depth the greater the attenuation.

The muon lifetime offers an opportunity for it to be tracked and measured in the detector. Muon neutrino CC reactions are sometimes referred to as "long" in comparison to the so called "short" NC reactions and tau and electron neutrino reactions. This can be complicated by relatively large muon backgrounds from cosmic ray muons, muons from the decay of pions and kaons, and possible charm decay products. Another advantage of the relatively long life is the ability to readily measure the muons charge and energy.

#### **4.2.3 Electron neutrinos**

Electron neutrino charged current reactions will produce a primary electron and possible hadronic showers. Since the electron does not decay, it will produce a shower of  $e^+, e^-$  particles and photons in the detector until all particles are absorbed. This absorption length will depend upon energy and the material through which the particles pass, but is nonetheless relatively short. The particles will deposit most of their energy early in the cascade. The transverse width of the electronic showers will be narrower than the hadronic NC showers.

#### **4.2.4 Hadronic showers**

In most all of the neutrino interactions, hadronic showers are a significant product of the reactions, either primary or secondary. Since these showers include mainly pions, kaons, and their decay products, it is not possible to distinguish the flavor of the original neutrino from the constituents of the shower. However, this can sometimes be accomplished statistically if the energies and momentums of the shower can be determined. The total energy spectra of NC reactions differ from CC reactions, and muon and electron spectra from tau spectra. Energy determination of both hadron and lepton showers will be necessary to determine the spectra of the incident neutrinos. In statistical analyses, energy cuts can sometimes be taken which will separate

and identify events based upon the hadron showers. Shower transverse momentum can also help determine the source of the shower, either as a NC reaction, from a CC reaction, or as a decay product.

### 4.3 Consequences

Statistical experimental methods are useful when direct, positive identification of a single particle reaction is not possible, or where background uncertainties and fluctuations obscure the actual results. Resorting to statistical methods means that larger data sets are required to get satisfactory results. This is due to the fact that the significance is proportional to the size of the detector. On the other hand a direct, positive identification of a particle reaction, which is background free, has a significance proportional to the detector mass or running time. For oscillation on the order of .01, a detector's sensitivity with direct identification approaches that of a detector that is thirty times more massive that uses an NC/CC test [ref\_sensitivity]. Therefore, first attempts should be made to accomplish direct identification by event.

Determining the identity of the primary lepton is essential to identifying the neutrino in CC reactions. Muons will be the most easily detected due to their long range and unambiguous decay. However, muons will be subject to backgrounds which may be large in comparison to the primary muon events. Electrons are best detected by methods which are capable of following the electronic shower to its conclusion. Otherwise, primary electrons may be easily confused with decays from other particles as well as other electron backgrounds. Taus will be the most difficult to detect directly since their decays occurs within 1 mm of their production and numerous decay channels are available. To see the initial tau, a detector resolution of approximately 1 mm is required. For the detection of the tau in NC reactions, a detector capable of analyzing the hadronic shower is required, but the method then becomes statistical.

Identification and sign determination of muons is a very important detection method. For muon neutrinos and electron antineutrino beams, so called *right* sign muons will be from non-oscillated neutrinos, while *wrong* sign anti-muons will be from oscillated neutrinos. The reverse will hold for  $\bar{\nu}_e$  and beams. This will provide a very useful statistical method for determining muon disappearance. In order to determine the charge, it will be necessary to have detectors with magnetic capabilities.

## 5 SPECIFIC DETECTOR TYPES

Neutrino detectors generally need to be large devices because of the small cross sections of neutrino reactions. Cost may dictate a choice between or a combination of large, less selective detectors vs. smaller, more selective detectors. Each detector needs to be designed with specific objectives in mind, as there is no single detector which will acquire all of the essential information needed to untangle the neutrino puzzle. Combinations of detectors are likely choices. A look at some of the possible detectors under consideration follows. In this proposal, we propose to study geologic engineering of siting specific detectors at WIPP, safety issues associated, and costing of the engineering. In the followings, we will look at various proposed detector options.

## 5.1 Water Cherenkov

The already large Super-K (50 kton) water Cherenkov detector [ref\_SuperK] could be scaled up by a factor of ten to twenty for use as a Far Detector for the neutrino factory beam. The main advantages of using water as the target medium are its low cost and relative transparency. Instrumentation would normally consist of PMT's located around the surface of the enclosed volume(s). In addition to more events, large containment volumes contribute to retaining fiducial event showers to the instrumented volume. The physics study group [ref\_Nuphysics] estimates that for a 50 kton water Cherenkov detector at 2900 km from a 10 GeV (muon energy in factory ring) neutrino factory, 57% of all muon CC events are fully contained, while at 50 GeV only 11% are fully contained. At the higher energies the numbers and complexities of identification and measurement of event showers increases dramatically. This leads to the conclusion that the water detectors must be large and probably operate at lower neutrino energies, possibly in the 10 GeV range. While the  $\nu_\mu$  event detection can be reasonably clean at 10 GeV,  $\nu_e$  event detection is much more problematic. Contamination from both  $\nu_\mu$  NC and CC and  $\nu_\mu$  CC events contribute to the background. Thus, the most useful neutrinos for water detectors to study will be muon neutrinos.

Charge determination of the primary leptons will be difficult for the water detector. Both internal and external magnetic fields have been studied. The internal approach suffers from field interactions on the PMT's. An external muon spectrometer may be feasible; however, muon acceptance decreases with lower neutrino energy. The solution may require breaking the fiducial volumes into smaller packages with more spectrometers.

## 5.2 Magnetized Fe Detector

### 5.2.1 Objectives:

The Magnetized Fe Far Detector may consist of two major components:

- (1) 50 kton of magnetized Fe, 8m sides and 500 m long, interleaved with tracking chambers to record production of muons and measure their charge and energy.
- (2) 4 kton of thin Pb and emulsion layers, in a configuration similar to that of the OPERA detector, to detect  $\tau$  production.

These large amounts of iron and steel could also act as a target for astrophysical neutrinos, and in particular offer the opportunity to obtain unique additional neutrino physics through observation of several thousand  $\mu$  and  $\tau$  neutrino events from a Galactic supernova burst. The additional instrumentation needed could be included without affecting the operation of the targets as a Far Detector.

The astrophysical neutrino signal would be produced by nuclear excitation of Pb and Fe nuclei, releasing neutrons, which can be detected by thermalization and absorption in a suitable detector. This process is sensitive predominantly to the higher energy  $\mu$  and  $\tau$  neutrinos, giving a signal

which complements the predominantly  $e^-$  anti-neutrino signal from the Super-K and SNO water detectors, and the LVD and the KamLAND scintillator detectors.

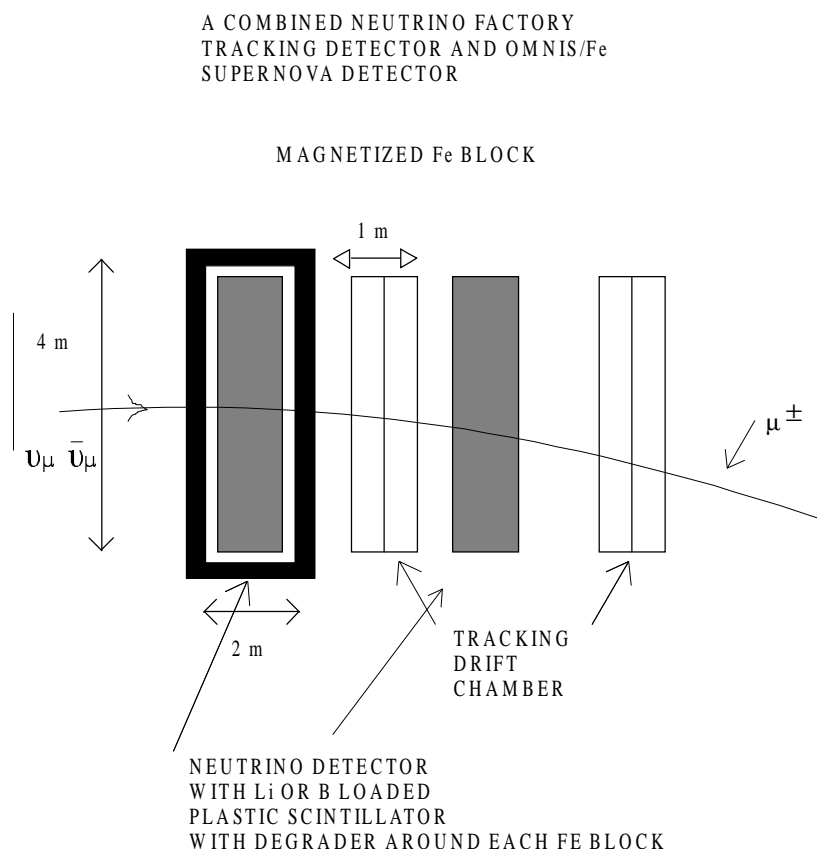


**Figure 2.** Magnetized Fe neutrino far detector for Neutrino Factory. The Fe blocks are interleaved with muon tracking drift chambers and neutron detectors for ancillary use of the Fe blocks for supernova neutrino detection.

The number and time profile of the events in both Pb and Fe targets provides limits on neutrino mass (down to a few eV) and measurements or limits on the  $\theta_{12}$  and  $\theta_{13}$  mixing angles through MSW production of higher-momentum electron neutrinos and consequent charged current excitation of the target nuclei. This also gives a distinctive two-neutron signal in the Pb target.

### 5.2.1 Detector Configuration and Signal Size

Efficient capture of neutrons is best achieved by means of alternating slabs of target and detector, with the target slab thickness typically 80-120cm in the case of Pb, and 20-30cm in the case Fe [ref\_Smith2]. In both the Fe and Pb cases, neutron-detecting planes can be inserted along the detector length with affecting the performance as a Far detector for charged lepton production. Figure aaa shows the result of Monte Carlo simulations of neutron captures (in a Gd + scintillator detector) from a supernova burst at 8 kpc, as a function of the distance between neutron detecting planes, referred to here as ‘module length’. Curves are shown for the typical case of 50 kton Fe and 4 kton Pb. The fall in events with increasing module length arises principally from the re-

absorption of neutrons by the target material before they can reach the detector. Figure 2 sketches the typical module structures of the combined detectors.

There are additional considerations, which may reduce the actual number of events detected, which we consider separately for the Fe and Pb targets:

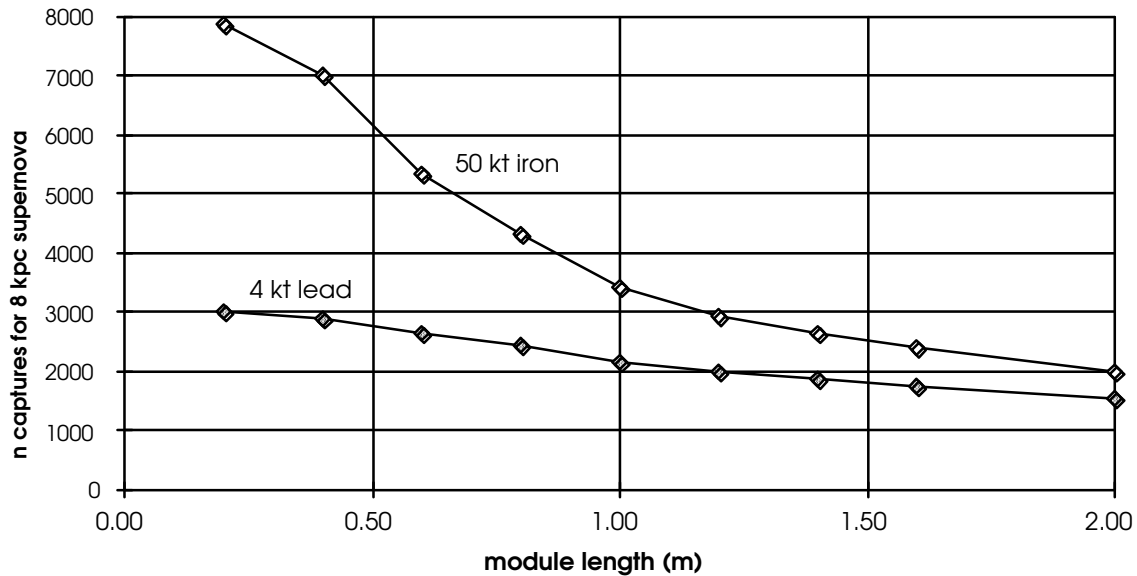


**Figure 3.** Neutron capture efficiency as a function of module length from simulation.

### 5.2.2 Fe target

The Fe curve in Figure xx shows that it is advantageous to insert neutron targets along the length more frequently than the muon detection intervals (typically 2m. Although a 2000 event signal could be obtained by including neutron detection in the same gaps as muon detection, one would gain a factor 2-3 in the supernova events by inserting neutron-detecting planes every 0.5-1m. Another factor affecting the detected signal is the gamma background from radioactivity in the Fe (mainly from U, Th and  $^{60}\text{Co}$ ). Since a Gd-based neutron detector relies on the subsequent gamma detection, this background can reduce the efficiency with which the neutron captures can be identified. An alternative technique based on absorption in thin sheets of LiF+ZnS is relatively gamma insensitive, but will still lose some of the neutrons in the separate moderator required. These losses will reduce the signal to typically 70-80% of those shown in Figure 1, but this still leaves a substantial supernova signal of 2000-40000 events at 8 kpc. Of course, the supernova distance effect is much greater than the instrumental effects, but one would like to ensure a several 100-event signal even from a supernova the other side of the Galaxy at 20 kpc.



## Far Detector + OMNIS: Fe configuration

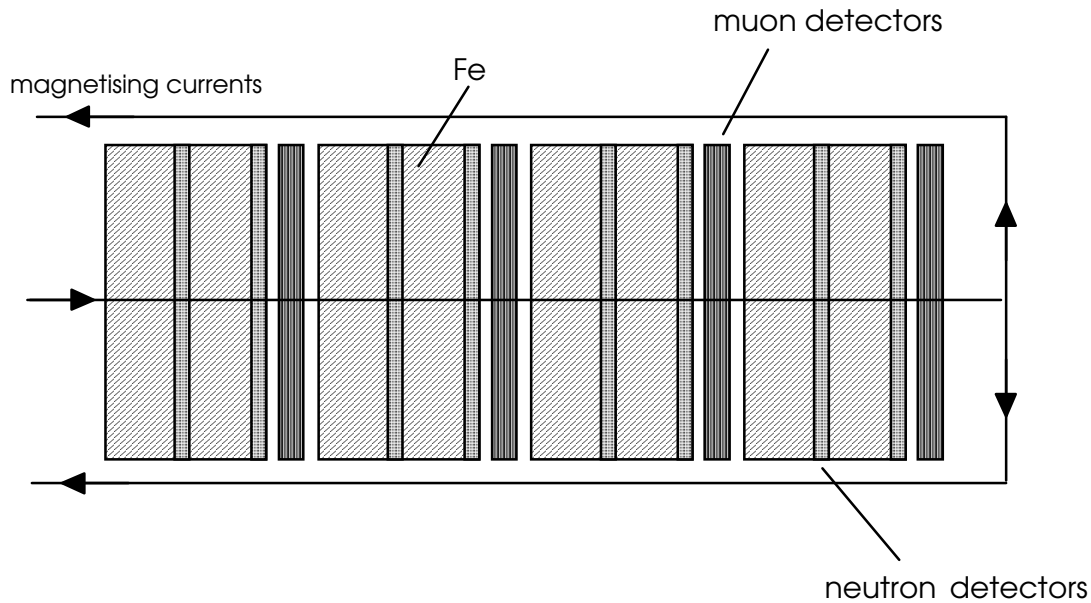


**Figure 4.** Far detector Fe configuration.

### 5.2.3 Pb Target

Figure xx shows the possibility of a 2000-3000-event signal from the Pb target, despite the much lower Pb mass. This is because (a) the neutron production in Pb is about 0.9 / ton compared with 0.2/ton for Fe, and (b) because Pb has a relatively low neutron absorption, allowing a higher fraction of neutrons to scatter out of the target to the detector. The longer neutron range also allows a 2000-3000 events signal from 0.5-1m spacing.

Attention has to be given to a complication arising from the more complex structure of the OPERA-based Pb/emulsion system. The gamma background from Pb is not an important effect in this case, since the U/Th contamination in Pb is typically about 2 orders of magnitude lower than in Fe. However, neutron losses can arise from the spacers in the finely subdivided multi-layer structure of an OPERA-based design. This has typically 1mm Pb plates adjacent to emulsion layers on 0.1mm plastic, separated by 3mm 'low density spacers'. If the latter were simply plastic at a density of  $1\text{g/cm}^3$  this would compete for neutron moderation and absorption with the 0.5-1m spaced neutron detectors. Ideally, therefore, these spacers should be made of a porous material of much lower density, and preferably minimum hydrogen content.

## Far Detector + OMNIS: Pb configuration

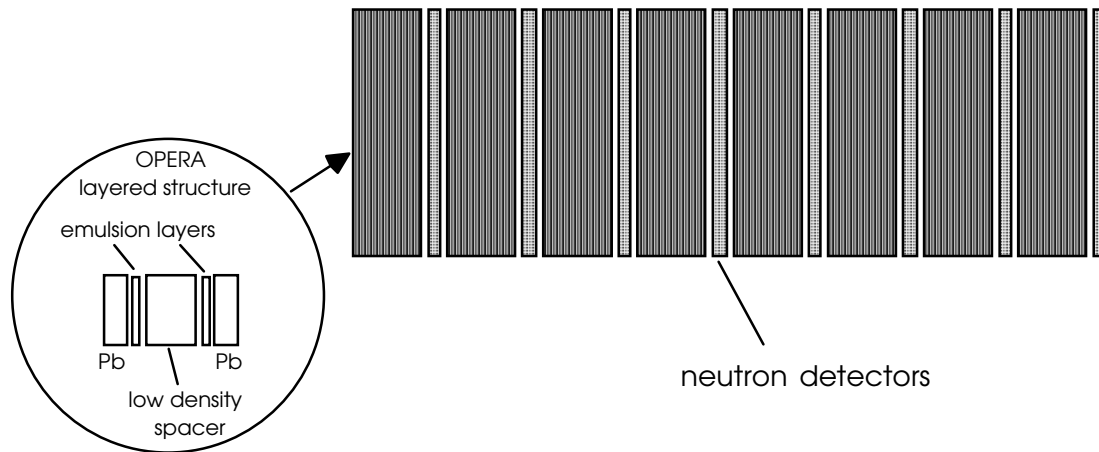


**Figure 5.** Far detector for Pb configuration.

### 5.2.4 Detector R&D

In this section, we identify areas of R&D needed for the neutron detectors. A number of neutron detection principles exist, all of which involve three components- moderation, absorption, and conversion to a signal. The moderator, absorber and converter can be combined or separate, leading to the classification of neutron detector types summarized in Table 3 and Figure xx.

The simplest option is type 1, consisting of a single combined material, available commercially as Gd-loaded scintillator and successfully used in other experiments. However, the Gd-loading makes it difficult to maintain long-term stability of the optical properties, and this makes it a doubtful candidate for a supernova detector operating for at least 10-20 years. There are two main alternatives:

- i) Use of Gd absorber in the type 4 configuration, in which a pure scintillator is used with adjacent solid slabs of Gd-loaded moderator. Simulations show that this has 80-90% of the efficiency of loaded scintillator, and has the merit of long-term stability of all the components [ref\_Smith1]. The use of Gd absorber has the disadvantage that a thickness of 20-25 cm of scintillator is needed to convert most of the Gd gammas, while the alternative of loading with  ${}^6\text{Li}$  or  ${}^{10}\text{B}$  (which release short-range nuclei) has not yet been achieved with reliable optical stability.
- ii) Construction of more compact detectors using the type 2 principle, in which a separate moderator is used, and  ${}^6\text{Li}$  or  ${}^{10}\text{B}$  are incorporated in a thin solid scintillator. Combinations of  ${}^6\text{Li}$  or  ${}^{10}\text{B}$  scintillating layers or fibers with moderators have been developed commercially [ref\_Bfibers] that is to be combined with a moderator by the user to suit the application. The unit cost is currently high for the commercial products, and would need to be reduced to the level of the simpler type 4 configuration.

These alternative options lead to the following R&D program:

#### Option (i)

A test program is required for the manufacture of the Gd-loaded moderator, and confirmation of its performance in conjunction with pure liquid scintillator. This requires a phase of laboratory tests, followed by an underground prototype assembly, including adjacent Pb or Fe walls and a neutron source, to simulate the neutron production, scattering, thermalization and absorption. The latter tests would be carried out in the Carlsbad underground facility in which the muon-induced neutron background is reduced by a factor  $10^5$  compared with that of a surface laboratory.

#### Option (ii)

A proposed starting point for the development of a slim type 2 detector would be the use of the already-available combination of  ${}^6\text{LiF} + \text{ZnS}$  [ref\_Lifibers]. After measurements of light output from individual neutron absorption, alternative planar readout options would be investigated, including Fresnel mirror systems and optical fiber planes, adjacent to the neutron-absorbing sheets. Outside of these two layers would be placed hydrogen-containing moderator panels. This multi-layer unit would be repeated to form an assembly a few cm thick.

Neutron source tests would be made on this moderator/detector assembly, to compare its detection performance with estimates from Monte Carlo simulations. As with options (i), an initial phase of tests can be carried out in the laboratory, but full tests with low neutron background require an underground prototype consisting of sheets of the composite detector sandwiched between shielding walls to assess the effect of radioactive backgrounds from both Pb and Fe. As in option (i) the use of the Carlsbad facility for these tests will ensure a neutron background reduced by a factor  $10^5$  compared with that at the surface.

### 5.3 Liquid argon TPC

The ICARUS detector proposed for Gran Sasso [19] in the CERN CNGS neutrino beam is a liquid argon time projection chamber (TPC) followed by a magnetic spectrometer and calorimeter. A TPC has the advantage of fine resolution and reconstruction of contained events and showers. The high resolution is responsible for an ability to identify and measure both electron-like and muon-like events. With the TPC all types of neutrino and antineutrino events can be reconstructed with varying efficiencies.

A similar TPC detector could be suitable for the WIPP site. The medium chosen for such large detectors should be linear in relation to energy, have a relatively long drift time, a high density, low recombination, and high transparency. Doping of the medium may also play a factor. Based on the ICARUS technology, a massive Liquid Argon Neutrino and Nucleon Decay Detector (LANNDD) has been conceptually designed recently to be sited at WIPP. It has tracking capability to see neutrinos from all directions and also simultaneously functions as a large volume of segmented high resolution nucleon decay search detector.

#### 5.3.1 Objectives:

- 1) Search for  $p \rightarrow K^+ + \bar{\nu}_\mu$  to  $10^{35}$  years lifetime
- 2) Detection of large numbers of solar neutrino events and supernova events
- 3) Study of atmospheric neutrinos

4) Use as a Far detector for a Neutrino Factory in the USA, Japan or Europe

### 5.3.2 LANDD Overview

One option for a next generation nucleon decay search instrument is a fine-grained detector, which can resolve kaons as well as background from cosmic ray neutrinos that are below the threshold for water Cerenkov detectors such as Super-Kamiokande (Super-K). Such a detector can make progress beyond the  $\text{few} \times 10^{33}$  years limits from Super-K for SUSY favored modes because the reach improves linearly with the time and not as the square root of exposure as in Super-K. This is because the background is low and the detection efficiency high. It will be possible to discover nucleon decay up to about  $\sim 10^{35}$  years lifetime per branching ratio with an instrument of  $\sim 70$  kton mass in liquid argon after a few years of exposure.

A second major goal for such an instrument, as demonstrated in a spectacular example of synergy in the last two generations of underground detectors, is the study of neutrino interactions and oscillations. Such a detector can make neutrino oscillation studies using the cosmic ray neutrinos alone (being able to resolve muon neutrino regeneration, to detect  $\tau$ 's and to tighten measurements of  $\Delta m^2$  search for other mixing than  $\nu_\mu \rightarrow \nu_\tau$ ). But coupled with a neutrino factory, this detector, outfitted with a large magnet, offers the advantage of being able to discriminate the sign not only of muon events, but of electron events as well. Given the bubble-chamber-like ability to resolve reaction product trajectories, including energy/momentum measurement and excellent particle identification up to a few GeV, this instrument will permit the study of the neutrino MNS matrix in a manner, which is without peer.

One may question whether such a marvelous instrument is affordable, by which we mean buildable at a cost comparable or less than the neutrino source cost. It is indicated by simple scaling from existing experience with ICARUS, that such an instrument will cost out in the class of a large collider detector instrument and represents a straightforward extrapolation of existing technology.

As expected for such a large, isotropically sensitive, general-purpose detector, there are many ancillary physics goals that can be pursued. This device would allow exploration of subjects ranging from the temporal variation of the solar neutrino flux (above a threshold of perhaps 10 MeV,) to searches for neutrinos from individual or the sum of all supernovae and other cataclysmic events, e.g. GRB's, to cosmic ray research on composition where the WIPP depth is advantageous, dark matter search via annihilation of neutrinos, searches for cosmic exotic particles such as quark nuggets, glueballs, monopoles, and free quarks, and point source neutrino astronomy. In all these instances we can go beyond Super-K by virtue of lower energy threshold, better energy loss rate resolution, momentum, angle, sign and event topology resolution.

We note that in the "Connecting Quarks with the Cosmos: Eleven Science Questions for the New Century" report for the National Academy, that such an instrument addresses eight of the eleven questions at least indirectly and of those eight, two explicitly for nucleon decay and neutrino mass.

### 5.3.3 The Carlsbad Site for LANNDD

In Figure 5, is a possible location of LANNDD at the Carlsbad Underground National Laboratory site (CUNL). Note that the ease of construction and the exhaust pipe are key motivations for this site. Safety would be accomplished by walling off the detector from the rest of the lab. Excavation is relatively inexpensive at this site due to the salt structure. However, engineering study needs to be carried out for costing.

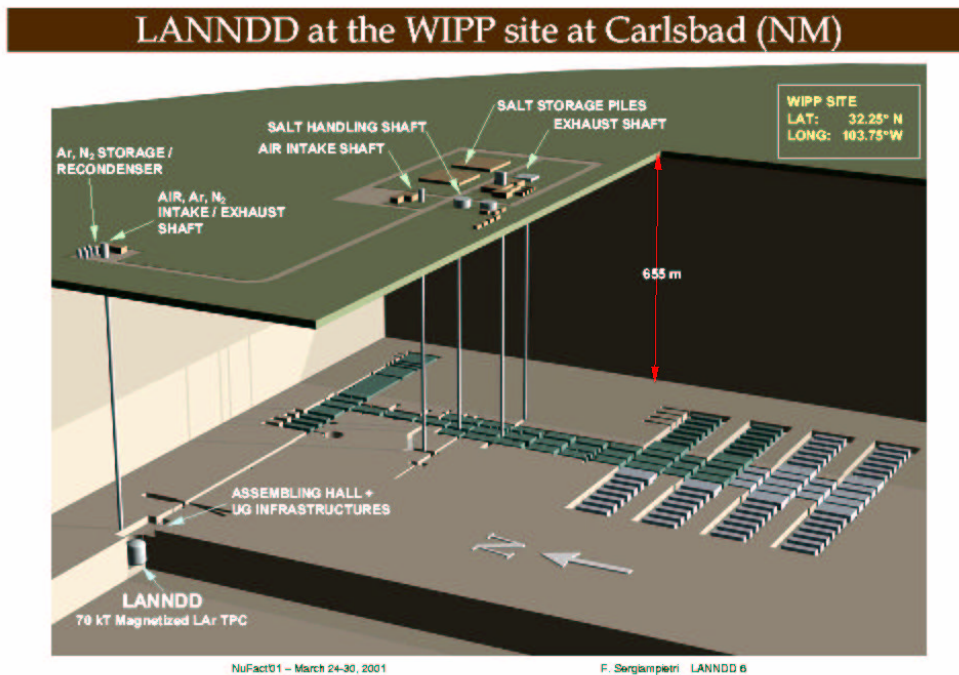


**Figure 6.** Liquid Argon Neutrino and Nucleon Decay Detector (LANNDD) shown located in the west end of the existing drift on the north side. The drawing shows the detector with its Argon filling and re-condensing system.

### 5.3.4 Some Scientific Goals of LANNDD

Much of the scientific studies to be done with LANNDD follow the success of the ICARUS detector program [ref\_ICARUS.]. The main exception is for the use of the detector at a neutrino factory where it will be essential to measure the energy and charge of the  $\mu^\pm$  products of the neutrino interaction. We will soon propose an R&D program to study the effects of the magnetic field possibilities for LANNDD.

a) Search for proton decay to  $10^{35}$  years

The detection of  $p \rightarrow K^+ + \bar{\nu}_\mu$  to  $10^{35}$  years lifetime

b) Solar neutrinos and supernova neutrinos studies



with  $\text{K}^*$  (Potassium-40) de-excitation giving subsequent gamma photoemissions. The same process is useful for supernova  $\nu_e$  detection --- the expected rate for the solar neutrinos is  $\sim 123,000$  per year. For a supernova in the center of the galaxy with full mixing there would be  $\sim 3000$  events --- no other detectors would have this many clean  $\nu_e$  events.

c) Atmospheric neutrino studies

By the time LANNDD is constructed it is not clear which atmospheric neutrino process will remain to be studied. However, this detector will have excellent muon, hadron and electron identification as well as the sign of the  $\mu^\pm$  charge. This would be unique in atmospheric neutrino studies.

The rate of atmospheric neutrinos in LANNDD will be (50ktons fiducial volume):

Electron Neutrino Events: 4800 per year

Muon Neutrino Events: 3900-4800 per year depending on the neutrino mixing

There would also be about 5000 neutrino current events per year. We would expect about 25 detected  $\nu_\tau$  events per year that all would go upward in the detector.

d) Use of LANNDD in a neutrino factory

Because of the large mass and nearly isotropic event response, LANNDD could observe neutrinos from any of the possible neutrino factories: BNL, FNAL, CERN or JHF in Japan. There are two approximate distances  $2-3 \times 10^3$  km and  $7-9 \times 10^3$  km for these neutrino factories. We assume the more distant neutrino factories to operate at 50 GeV  $\mu^\pm$  energy. For a neutrino factory that produces  $10-20 \mu^\pm$  per year at FNAL or BNL and expect  $\sim 50,000$  per year of right sign muons, i.e.  $\mu^+ \rightarrow e^+ + \nu_e + \bar{\nu}_\mu$  and detection of  $\mu^+$  via charged current conversion.

The number of wrong sign muons will depend on the mixing angle  $\theta_{13}$  where in the above reaction  $\bar{\nu}_\mu$  converts into  $\nu_\mu$  and the subsequent detection of  $\mu^-$  via charged current. There could be as many as 5000 wrong sign events per year.

For the farther distances (CERN to Kamioka), these numbers would be about the same due to the higher energy  $\mu^\pm$  of 50 GeV with the rate increasing as  $\sim E_\mu^3$ .

The LANNDD detector could be useful for the search for CP violation from any neutrino factory location. This will depend on the value of the mixing angle  $\theta_{13}$  and the magnitude of the CP violation.

For the longer distance experiments (CERN to Kamioka), there could be an important MSW effect that is important to study in order to evaluate the significance of the CP violation search. It is possible that the electric charge of the  $e^\pm$  from the reaction  $\bar{\nu}_\mu \rightarrow \bar{\nu}_e$  could be determined as it was in heavy liquid bubble chambers by following the shower particles---this is currently under study.

In Figure 2, we show the schemata of neutrino factory beams to the CUNL site for detection by LANNDD---we consider this a universal neutrino factory detector.

### 5.3.5 Detector

The aim is to build a 70-kton active volume liquid argon TPC immersed in magnetic field. The geometric shape of the detector is mainly decided by the minimization of the surface-to-volume ratio  $S/V$ , directly connected to the heat input and to the argon contamination. Spherical (diameter= $D$ ), cubic (side= $D$ ) or cylindrical (diameter=height= $D$ ) shapes have all the minimum  $S/V = 6/D$ . As a compromise between easy construction and mechanical stability, the cylindrical shape has been preferred. Adding to the  $S/V$  criterion the need of minimizing the number of readout wires and of maximizing the fiducial-to-active volume ratio, a single module configuration appears definitely advantageous with respect to multi-module array configuration (see Table xx). The more difficult mechanical design for the single volume configuration appears fully justified by the larger fiducial volume, the lower number of channels, the lower heat input and contamination and then lower construction and operating costs.

	1 Module	8 Modules	64 Modules
Active Volume (m <sup>3</sup> )	50,000	50,000	50,000
Fiducial Volume (m <sup>3</sup> )	41,351	33,559	21,037
Number of Channels	164,261	337,787	724,077
Heat Input (Watts)	9,104	18,209	36,417

**Table 1.** Comparison is made for single module and many modules.

The internal structure of the detector is mainly designed to the maximum usable drift distance. This parameter depends on the acceptable attenuation and space diffusion of the drifting charges. Acceptable working conditions are obtained with an electric field of 0.5 kV/cm, a drifting electron lifetime of 5-10 msec and a maximum drift of 5 m. The detector appears then as sliced into 8 drift

volumes (Figures 2,3), 5 m thick, each confined between a cathode plane and a wire chamber. Each wire chamber is made of two readout planes (u,v) with wires oriented at  $+45^\circ$  and  $-45^\circ$  with respect to the horizontal plane. A 5 mm wire pitch gives a sufficiently detailed imaging of ionizing tracks in the drift volumes.

The magnetic field is vertically oriented and is obtained with a solenoid around the cryostat containing the liquid argon. With such an orientation the maximum bending for a charged particle is obtained in a horizontal plane and appears in the imaging as an arc in each of the planes (u,t) and (v,t).

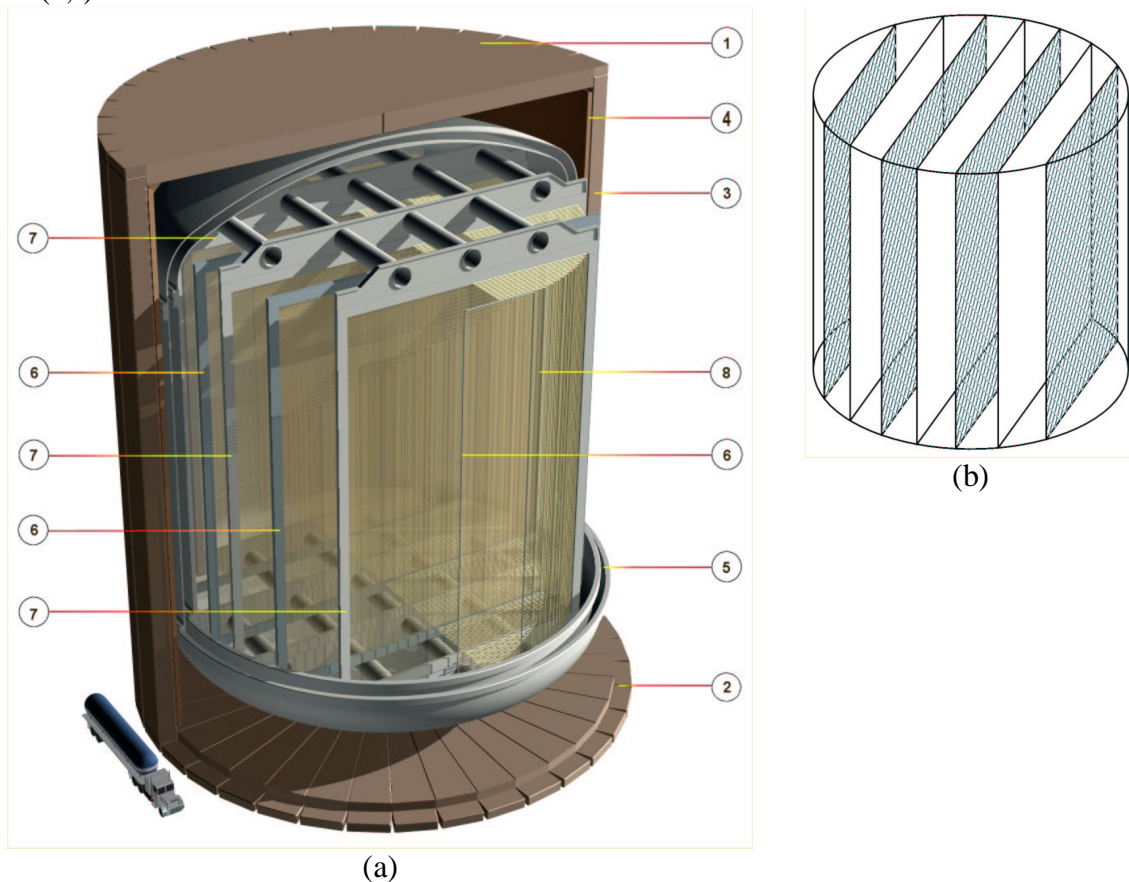


**Figure 7.** (a) Preliminary sketch for LANNDD: 1) Top end cap iron yoke; 2) Bottom end cap iron yoke; 3) Barrel iron return yoke; 4) Coil; 5) Cryostat; 6) Cathodes; 7) Wire chamber frames; 8) Field shaping electrodes. (b) Schematic layout of chamber (hatched regions) and cathodes planes (white regions).

The detector is foreseen as located underground as shown in Figure 5, at a depth of 655 m (2150 ft) in a housing equipped with an emergency liquid argon pool and with argon vapor exhaust ducts. Forced fresh air inlet, liquid/vapor nitrogen in/out ducts, assembling hall with crane and elevator complete the basic organization of the underground cave. The magnetic field is vertically oriented and is obtained with a solenoid around the cryostat containing the liquid argon. With such an orientation the maximum bending for a charged particle is obtained in a horizontal plane and appears in the imaging as an arc in each of the planes (u,t) and (v,t).





system; (b) Additional details on the assembling and storage hall.

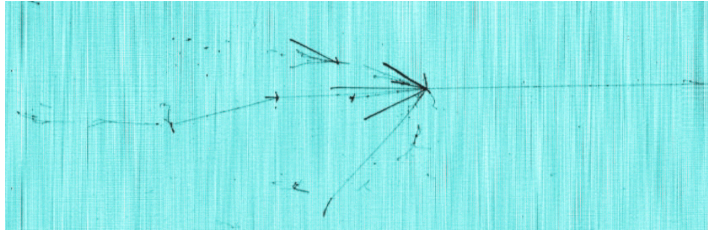


**Figure 9.** One of the first images of cosmic muon shower recorded recently by the liquid Argon detector ICARUS.

### 5.3.6 Preliminary study in view of a detailed project for the LANNDD detector at the WIPP site

Extra large active mass detectors, as required by the experimental study of neutrino oscillations made with long baseline neutrino beams, are also the ideal source for the search of the lower limits for the nucleon lifetime. A detector, based on the liquid argon time projection chamber (TPC) configuration, appears particularly appealing for its homogenous (in space) and continuous (in time) sensitivity. Its 3D “imaging” capability and its calorimetric performance make this kind of detector unique for event reconstruction in the finest detail even at very low energy. The cosmic background suppression requires siting such a device underground. The possibility to operate this detector in magnetic field widens its detecting power especially in neutrino oscillation experiments made with beams generated by neutrino factories.

A preliminary study has been performed<sup>1</sup> to put in evidence a set of guidelines for the design of such an apparatus, based on requirements and constraints mainly originated from the experience accumulated in the design and operation of smaller scale similar detectors. Such criteria and remarks are mainly dictated by the user (physicist) point of view. The solution resulting from this study is a kind of challenge that need to be certified by a detailed complementary study, made by the engineering point of view, covering issues connected to the mechanical stability of the chamber supporting frames, of the cryostat and of the magnet and to their safe siting, assembling and operation in an underground environment. Mining technology criteria and related safety constraints must be taken into account for the design of the underground cavern, capable to host a clean laboratory, with proper ventilation, access and other services. Even if argon is an inert gas, its use in liquefied state, in large quantities and in an underground site requires particular precautions and coherence with the related safety rules. Surface infrastructures for liquid argon and nitrogen production will be considered. Finally, the electric power consumption, mainly connected to the operation of the magnet, must be evaluated.

As working hypothesis we have assumed to design a detector *a*) with active mass of 70'000 tonne (70 kT), *b*) sited at the WIPP underground laboratory (NM) and *c*) eventually immersed in a magnetic field.

The main items to be considered are the subject of the following sections.

---

<sup>1</sup> D. B. Cline, J. G. Learned, K. T. McDonald and F. Sergiampietri, *LANNDD - A Massive Liquid Argon Detector for Proton Decay, Supernova and Solar Neutrino Studies and a Neutrino Factory Detector*. Proceedings of the NUFAC'01 WORKSHOP, Tsukuba, Ibaraki, Japan, May 24-30, 2001; Astro-PH/0105442.

#### a) Shape and modularity

A cylindrical shape, with height approximately equal to the diameter, appears as an optimal choice if omni-directional sensitivity is required together with a minimum surface-to-volume (S/V) ratio. If the cylinder is oriented with vertical axis and is equipped with top and bottom toro-emispherical shells, this shape appears promising from the point of view of the mechanical stiffness and of the easy design of the internal detector electrodes (compare with spherical and cubic shapes that have the same S/V ratio).

The S/V ratio is the deciding criterion for a choice between configurations based on a single large unit or on an array of equal, smaller modular units. The following parameters depends roughly linearly on the inverse of the linear size of modules:

- Number of channels (i.e. wires, wire combs, connectors, cables – and heat input through them –, signal feedthroughs, electronic chains, data acquisition and storage power. By excluding the magnet, the most important fraction of the total detector cost results proportional to the number of channels)
- Impurities
- Heat input (cooling power)
- Magnetic power
- Magnet coil weight

Other important parameters depend on the inverse of the size of modules, even if less than linearly:

- Active/fiducial volume ratio
- Magnet iron yoke weight

The above parameter dependences, that qualify the detector and determine its cost, suggest without any doubt the choice for a single module configuration. The resulting active volume size is roughly a cylinder 40 m in diameter, 40 m in height. These sizes are still realistic for the liquid argon TPC operation (consider, per example, that a 40 m long wire with 3 mm wire spacing, as those in the wire chamber planes, has an electrical capacitance of  $\sim 800$  pF, for which the equivalent noise energy is of the order of 40 keV rms, while the energy deposited along the 3 mm wire spacing is, at minimum, 2.1 MeV). On the other side, the practical feasibility, in safe conditions, of this configuration is matter for an engineering study and evaluation.

#### b) Insulation

Considering that the outer cryostat surface is of the order of  $8000\text{ m}^2$ , a heat input of  $1\text{ W/m}^2$  (corresponding to a liquid nitrogen evaporation rate of  $0.64\text{ l/m}^2/\text{day}$ ), the total liquid nitrogen consumption amounts to  $5\text{ m}^3/\text{day}$ . The vacuum insulation appears as the ideal technique for the thermal shielding of the cryostat. Heat input rates of the order of  $\leq 0.5\text{ W/m}^2$  are commonly reached with such technique combined with a coating of superinsulation layers (average conductivity  $\lambda_{90^\circ-300^\circ\text{K}} = 4 \cdot 10^{-5}\text{ W}\cdot\text{m}^{-1}\cdot\text{K}^{-1}$ ). While techniques based on expanded foams or other solid-state insulators are generally 20-100 times less efficient (for expanded foams of polyurethane, polystyrene, PVC the average conductivity is  $\lambda_{90^\circ-300^\circ\text{K}} = 2.5 \cdot 10^{-2}\text{ W}\cdot\text{m}^{-1}\cdot\text{K}^{-1}$ ; for honeycomb panels in aramid fiber, filled with nitrogen gas – as for the ICARUS cryostat –, it results  $\lambda_{90^\circ-300^\circ\text{K}} > 10^{-1}\text{ W}\cdot\text{m}^{-1}\cdot\text{K}^{-1}$ , with a heat input of the order of  $20\text{-}40\text{ W/m}^2$ ).

Particular design solutions must be adopted to cope with the required safety and ensure the required stiffness and reliability of the cryostat wall. With large sizes, one of the main points to take into account is the thermal shrinkage of the inner walls, compared to the outer walls.

### c) Magnetic field

The physics requirements for immersing the LANNDD detector in magnetic field are related mainly to the study of neutrino oscillations. Preliminary calculations indicate that, for charge-sign discrimination, a magnetic field intensity of  $0.2 T$  is suitable for muons while  $1 T$  is required for electrons (if their energy is lower than  $10 GeV$ ). The decision of the field intensity is then related also to the perspectives on future long baseline beams and on their energy distributions.

A second matter to discuss is the choice between warm and superconducting coil.

Finally a decision must be taken on the relevance of outfitting the coil and the cryostat, inside it, with an iron return yoke. The mass of the iron required at  $0.2 T$  is of the order of 120 tonne (247 tonne for  $0.4 T$  and 677 tonne for  $1 T$ ). A solution without yoke implies special precautions to be observed and an accurate choice of non-ferromagnetic materials for any infrastructures and facilities in the underground hall.

The possible integration of the eventual iron yoke in the pit walls and as link to the cryostat outer vessel must be studied.

Preliminary studies for a warm magnet with maximum field of  $0.2 T$  indicated a power consumption of about  $17 MW$  ( $37 MW$  at  $0.4 T$  and  $79 MW$  at  $1 T$ ). This estimate is obtained by equilibrating the copper cost with the power cost during 10-year operation.

### d) Underground

A tectonic and geological survey is required. Rock solidity and stability must be verified as suitable to carry a pressure load of  $50\text{-}100 \text{ tonne/m}^2$  distributed over an area of about  $2000 \text{ m}^2$ . The basic configuration of the LANNDD underground laboratory should include a barrel vault hall (used, initially, for preparation and intermediate assembly of detector details, and later for hosting cryogenic and purification devices) and a well in the hall floor where the detector will be located. By this configuration, due to the density of argon higher than the air density, in case of leakage, the argon will concentrate in the bottom of the well.

Upcast shaft for argon vapor exhaust and downcast shaft for fresh air intake, both with properly sized fans, are needed to face eventual important liquid argon leaks. The argon shaft is connected to a toroidal duct surrounding the lower base of the well, while the fresh air shaft is connected to a similar duct around the upper part of the well.

Thermally insulated pipes are required for liquid argon and liquid nitrogen transfer from the surface cryogenic plant to the cryostat, for filling (liquid argon) and cooling/stabilizing (liquid nitrogen) the cryostat. The (vertical) transfer pipes, equipped with adequate intermediate stations for hydrostatic pressure reduction, are combined with auxiliary larger section pipes for vapor exhaust. The pipe for argon vapor is utilized as safety expansion volume for eventual liquefied argon pressure compensation.

A mobile bridge crane is required in the underground hall to lift semi-assembled details in the detector well for final assembling.

The hall should include a closable hut, usable as electronic counting room and as emergency safe volume. Connected to it, a lift for people should be foreseen.

The hall must be designed to foresee, at the moment of the final detector assembly, a clean box as access to the detector, with people properly dressed for clean room operation.

### e) Surface infrastructures

A set of services and infrastructures has to be foreseen in an area on the surface on the vertical from the underground well:

- A liquid Argon/nitrogen plant to economically produce the liquid argon to fill the detector and the liquid nitrogen for cooling and stabilizing in temperature.
- A mechanical yard equipped with a semi-fixed crane for the detail construction and for their moving down through the fresh air emergency shaft (initially used for this purpose).
- An electric power sub-station.

#### f) Conclusions

The construction of an apparatus characterized by a 70 kT sensitive mass is mainly an engineering task. The principal guidelines dictated by physics and detector considerations have been introduced. A preliminary technical study aimed to freeze the general strategic choices on the detector configuration, its magnet and its underground siting is highly required.

### 5.4 Nuclear emulsion

Nuclear emulsion detectors on a scale much smaller than one required for a neutrino factory have been used in CHOOZ and are planned for OPERA [ref\_OPERA] and MINOS [ref\_MINOS]. The concept of a large (1 kt to 20 kt) detector with nuclear emulsion planes sandwiched with steel plates and low-Z gaps inside a large toroidal magnet has been proposed. Such a detector would allow identification (including charge) and energy measurement on an event-by-event basis of all primary lepton types.

Nuclear emulsion detectors are very fine grained and provide complete reconstruction of contained events. This might allow them to be somewhat smaller than other detector designs while still remaining effective. Real time data acquisition through automated microscopic digitizers have been demonstrated (CHORUS) to simplify data gathering.

Nuclear emulsions have the disadvantage of high cost.

### 5.5 Others

Other detectors that have been mentioned in the literature [ref\_Nuphysics] are perfluorohexane (C<sub>6</sub>F<sub>14</sub>) filled Cherenkov detectors and microstrip gas chambers. Both are noted as being effective for the specific detection of tau particles.

### 5.6 Detector considerations

Experimental detectors will experience the highest interaction rates with oscillated neutrinos if they are located at source distances at or near the leading oscillation maximum; however, distances greater than the first oscillation maximum complicate interpretation since it can be uncertain upon which oscillation cycle the detector is located. The vacuum oscillation length for one cycle is a function of the ratio of the neutrino energies in the beam  $E_\nu$  in GeV and the mass difference squared  $\Delta m_{ij}^2$  in  $\text{eV}^2/c^4$ ,

with  $L$  in km [ref\_Geer]. At present the best determination of  $\Delta m_{ij}^2$  is  $3.5 \times 10^{-3} \text{ eV}^2/c^4$  from

Super-K. The present best value of  $\sin^2(2\theta_{23})$  is 1 and also comes from Super-K.  $\sin^2(2\theta_{13})$  is not well determined, but the best value comes from CHOOZ with  $\sin^2(2\theta_{13}) \sim 0.047$  [ref\_CHOOZ]. Muon neutrino to tau neutrino vacuum oscillations, using these parameters, will have the first oscillation maximum at approximately 4,960 km for a  $E_\nu$  of 14 GeV (the rough equivalent of 20 GeV muons in the factory storage ring). Oscillation probabilities of the other neutrinos will be lower, but the oscillation lengths will be the same. Matter oscillation lengths will be on the order of 10,000 km for ordinary rock with a density of around  $3.0 \text{ g/cm}^3$ . While matter oscillations are not dependent on neutrino energy, the combined vacuum/matter oscillations are dependent.

Intense  $\nu_\mu$  beams will produce a comparatively large flux of muons by interacting with the rock (salt) in advance of the detector. These muons will create a significant background in the detectors. Placing a powerful magnet between the detector and rock face could steer muons away from the detector and lower this background.

By utilizing two identical far detectors at radically different locations or one detector receiving identical beams from two factories at different distances, such as WIPP from Fermilab or BNL and WIPP from CERN or Gran Sasso from CERN and Gran Sasso from Fermilab or BNL, it may be possible to consider somewhat smaller detectors. Many of the uncertainties related to the beam, the detector, and cross sections could be removed through ratios. For example, the ratio of any of equations (4) through (6) for different combinations of factory-detector lengths drops out the  $\sin^2\theta_{13}$  dependencies, leaving  $\Delta m_{32}^2$  as the only variable. Furthermore, all three equations result in the same variable. It would be possible to ratio equations (4) and (5) at the same or different factory-detector combinations to zero in on  $\sin^2(2\theta_{23})$ . Such a start would assist in the unravelling of the other parameters in a manner more direct than curve fitting. Care must be taken in selecting the data with the best statistics for this purpose, as ratios can increase the error ranges.

Where two detectors are not available for a given beam, it is possible to run two different experiments with one detector but with different beam energies. The equations will ratio in the same manner; however, the different energies will introduce some systematic error since beam spectra and cross sections will be different and perhaps not well known.

Whatever primary neutrino detector is chosen for a factory neutrino beam, magnetic spectrometers and calorimeters should be included in the mix. These will likely be located at the ends of multiple modules or, if the modules are small enough, the entire modules may be located within magnetic fields. Furthermore, it may be desirable to combine more than one type of primary detector, such as a magnetized steel/scintillator of large mass and nuclear emulsion detector or liquid argon detectors of a smaller mass. If CP violation is to be studied, it will probably require some form of tau detection.

## 6 DETECTOR PROPOSAL

i) Tunneling in the salt at a large angle for alignment of detector towards the neutrino source. This could require engineering study of the salt formation.

- ii) Configuring the detector to run in parallel as an OMNIS detector.
- iii) Cost and time scale of tunneling and the detector.

This paper presents a proposal for the study of a remote detector to serve with a neutrino factory or superbeam to study long baseline oscillations of neutrino flavors. The study will focus on physics benefits, detector design, neutrino detection methods, simulation of the experiment, the results expected from the experiment, and future upgrades possible for the experiment.

The neutrino factory location is unknown, but for purposes of this study it will be assumed to be located either at Brookhaven National Laboratory or at Fermilab, eventually perhaps both. There may also be future neutrino factories in Europe or Japan. The beam parameters to be used in this study will be the Fermilab parameters as addressed previously. However, during the course of the study if more favorable parameters are provided by either Fermilab or Brookhaven, the revised parameters may be substituted. Although it is probable that there will ultimately be more than one detector location in the world, this study will be concentrated on a detector located at the Carlsbad National Underground Laboratory. This National Laboratory provides all of the needed components for the location of a world class neutrino detector.

## **6.1 Detector location**

The multiple factory, single detector approach taken here will allow for comparisons to be made using the final study data, which ultimately may have a bearing on final factory site selection. In addition, the study will look at longer baseline experiments from a potential neutrino factory located at CERN near Geneva, Switzerland.

Some detectors and experimental scenarios are more sensitive to the muon flux from cosmic rays than are others. Since the factory beam is pulsed, it is possible to obtain a good value of cosmic ray backgrounds during the dead time, which can then be subtracted from the live events. However, to keep the statistical fluctuations of the background low, it would be prudent to have a deep enough experimental site, at least of the order of 2000 mwe.

Neutron background flux from uranium or thorium in the surrounding strata could be a problem for detectors using NC reactions and neutron signals for the detection mechanism. If neutron levels were high enough, supplemental shielding might be required. How important neutron backgrounds are would have to be evaluated for each type of experiment considered.

The Waste Isolation Pilot Plant (WIPP) in Carlsbad, New Mexico, has been designated by the Department of Energy as a national scientific underground laboratory, named the Carlsbad Underground National Laboratory (CUNL). There has been intense interest recently among the scientific community in establishing a national underground laboratory for neutrino and other experiments. For neutrino oscillation studies, the most important criteria for locating a detector are its distance from the neutrino factory, reasonable underground depth to avoid cosmic ray backgrounds, low radiation backgrounds from the surrounding underground strata, and a well developed infrastructure to support the experimentation. Distances which approximate the first vacuum oscillation maximum would be preferable. Since the parameters used to calculate this

distance are not well known, the best available values have been used. At present this distance would be 2450 km for 7 GeV neutrinos, ranging up to 12,250 km for 35 GeV neutrinos. The neutrino detector for this will be located at the CUNL in Carlsbad, New Mexico.

### 6.1.1 Carlsbad Underground National Laboratory

The Waste Isolation Pilot Plant (WIPP) located near Carlsbad, New Mexico, has been established by the Department of Energy for use as a United States underground laboratory facility using the name Carlsbad Underground National Laboratory (CUNL). Such a facility would be a favorable site to locate a detector for a neutrino factory. At a recent workshop on *WIPP as the Next Generation US National Underground Research Facility* held in Carlsbad, New Mexico, on June 12-14, 2000, a collaboration was announced for design and development of a detector for neutrino factory beams at WIPP. Among the collaborators are representatives from UTD, UCLA, LANL, DOE/WIPP, TAMU, TAMU-Kingsville, and Princeton. This proposal results from that collaboration.

Factory Site	To CUNL (km)	$E_\nu$ ( GeV) at 1st Max
FNAL	1,749	4.9
BNL	2,903	8.2
CERN	8,136	23.0

**Table 2.** Distances to the CUNL site from likely locations of neutrino factories.  $E_\nu$  corresponds to the first oscillation maximum for each distance.

The CUNL site is located such that it can be on the first vacuum oscillation maximum from Fermilab, Brookhaven, or CERN by using a mean beam energy that is available from the neutrino factory. The parameters values used may differ from actual values; however, adjustments of neutrino energy can change where the detector falls on the oscillation cycle, making it possible to enhance oscillations at the detector. The Fermilab and Brookhaven distances have the advantage of low values for matter oscillations, thereby making analysis of the vacuum oscillations easier to isolate.

The CUNL site has other qualities which make it a good location for this detector. The underground laboratory site is presently 655 meters below the surface, with a possible increase to 1300 meters. Cosmic radiation shielding at these levels are estimated at 1,840 and 3,524 mwe (taking into account flat surface and muon angular distribution). The material from which the laboratory is excavated is rock salt, which in comparison to rock, is much less expensive to excavate. The salt contains low levels of radioactive elements; uranium 30-50 ppb, thorium 70-80 ppb, and potassium-40 0.1-0.8 ppm. Free neutron levels have been measured at  $332 \pm 148$  neutrons/m<sup>2</sup>/day with thermal and epi-thermal neutron flux levels at  $115 \pm 22$  neutrons/m<sup>2</sup>/day. Radon concentrations are at surface air concentrations since the facility is provided with large quantities of fresh circulating air. The site is operated by the US Department of Energy, which maintains a large infrastructure of power, lighting, elevators, and surface facilities along with operational, safety, security, and environmental services.



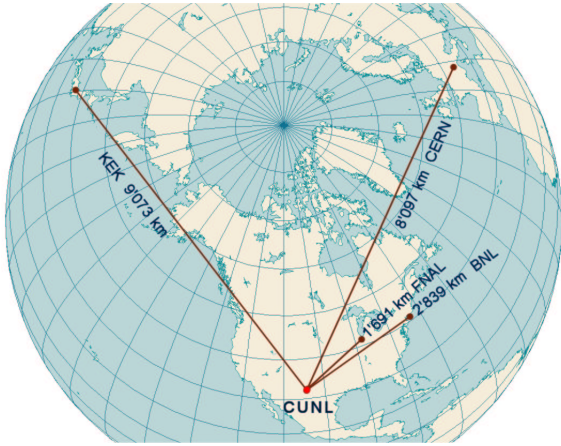


**Figure 4.** Distances to Carlsbad Underground National Laboratory (CUNL) from respective world accelerators where neutrino factory can be built.

Long Baseline Beam	Distance to CUNL (km)	$\theta_H$	$\theta_L$
FNAL	1,691	+47.9°	+ 7.8°
BNL	2,839	+62.5°	+12.9°
CERN	8,097	+41.6°	+39.5°
KEK	9,073	-44.7°	+45.4°

**Table 3.** Distances and angles to Carlsbad Underground National Laboratory (CUNL) from respective world accelerators.

## 6.2 Detector design

It is assumed from the start that any detector that is built, along with a neutrino factory, must meet certain cost constraints. The approach to be taken in this study will be to design a cost efficient initial detector, that can be augmented with additional detectors, modules, electronics, etc. in the future to expand its initial capabilities. The possibility of using this detector for astrophysics studies on solar, atmospheric, supernova, extra-galactic, and relic neutrinos will be considered.

All detector types as presented above will be considered as candidates for further study; however, a single detector type will be selected for more detailed study. For example, a first detector type could be a 10 metric kton collection of iron plate targets, sandwiched with electronic particle detectors. These particle detectors could be arrays of scintillating plastic or liquid scintillation detectors with scintillating fiber readouts. Electromagnets would provide for a toroidal magnetic field in the steel plates. This detector would have properties very similar to the MINOS detector. A detailed study would arrive at a final design after applying the results of experimental simulations. It would not be the intent of the study to enter into the detailed engineering design of the detector, beyond establishing general parameters.

The size of size of such a detector and number of identified reactions is especially important for those detectors relying on statistical methods of identification such as the one described above.

To give an indication of the number of events that could be recorded in this detector, Table 3 lists the number of events expected in one year of operation for the 10 kt detector at CUNL with the factory at Fermilab. The neutrino beam is taken as the Fermilab flux of  $6 \times 10^{19}$  muon neutrinos and (electron antineutrinos) per year at an energy  $E = 14$  (12) GeV. The neutrino oscillation parameters are  $\sin^2(2\theta_{13}) = 0.47$  and  $\sin^2(2\theta_{23}) = 1.0$ . For other factory-detector combinations the number of events will be almost inversely proportional to the square of the distances.

$\Delta m_{32}^2$	$P(\nu_{\mu} \rightarrow \nu_e)$	$P(\bar{\nu}_{\mu} \rightarrow \bar{\nu}_e)$	$P(\nu_{\mu} \rightarrow \nu_e)$	$P(\bar{\nu}_{\mu} \rightarrow \bar{\nu}_e)$	$\nu_e$	$\nu_{\mu}$	$\nu_{\tau}$	$\bar{\nu}_e$	$\bar{\nu}_{\mu}$	$\bar{\nu}_{\tau}$
.000	.0000	.0000	.0000	.0000	0	<b>14,134</b>	0	<b>6,057</b>	0	0
.001	.0012	.0236	.0017	.0017	18	<b>13,818</b>	80	<b>6,037</b>	10	2
.002	.0049	.0920	.0065	.0065	69	<b>12,902</b>	312	<b>5,978</b>	40	9
.003	.0105	.1984	.0139	.0139	148	<b>11,477</b>	673	<b>5,889</b>	84	20
.004	.0175	.3323	.0227	.0227	248	<b>9,685</b>	1127	<b>5,782</b>	138	33
.005	.0253	.4804	.0319	.0319	358	<b>7,703</b>	1629	<b>5,671</b>	193	46
.006	.0331	.6278	.0401	.0401	468	<b>5,729</b>	2130	<b>5,572</b>	243	58

**Table 4.** Probabilities and number of events for a  $\mu^-$ -decay beam for various values of  $\Delta m_{32}^2$  assuming oscillations with  $\sin^2(2\theta_{13}) = 0.47$ ,  $\sin^2(2\theta_{23}) = 1.0$ ,  $E_{\mu} = 20$  GeV and  $L = 1749$  km. Bolded events are from non-oscillated neutrinos.

### 6.3 Detection methods

This study would consider the physics inherent in different detection methods to arrive at a set of procedures which can be simulated using Monte Carlo methods. These procedures follow from the discussions of sections 4 and 5 of this paper. The procedures would consider actions such as taking prudent energy cuts for the elimination of background, finding methods to eliminate or minimize systematic errors, or using mathematical tools such as ratios to enhance calculations from the data sets obtained. The procedures will be designed with regard to increasing the significance of the statistical data where possible.

### 6.4 Simulations

Based upon the procedural methods chosen for particle detection, sets of simulations using different parameters of the beam, factory-detector combinations, and neutrinos will be run in order to (1) optimize the beam running energy, (2) optimize the detector design and parameters, and (3) arrive at a final set of predicted experimental results. The predicted results would be used as the templates for comparison with actual experiment results in the final calculation of neutrino parameters or in establishing new limits of the neutrino parameter spaces.

The simulation program which would be appropriate for this study would be the GEANT4 detector program, available from CERN. Special code will have to be written to fit these experiments into GEANT. Other specific programs used in the particle physics experimental community may also be used. The GEANT4 program is available for use with either the UNIX or

Windows operating systems. Since programs of this complexity require considerable computer capacity, it will be necessary to use an appropriate computer, e.g. the UCLA or UT System central computers.

## 6.5 Detector Summary

Neutrino experiments are presently a very important part of experimental physics, both from a particle physics aspect and astrophysics. Neutrino factory and detector experiments, similar to the one described in this proposal, are likely to be undertaken in the next ten to fifteen years. The results that come from this proposal should benefit in the planning of such experiments. The procedures developed and the simulations run should be able to provide significant guidance in the final design. Should the final experiments be similar in nature to those proposed here, the simulations could become templates for comparison and calculation of the neutrino parameters being sought.

	Baseline length (km)		Vertical Angle <sup>a</sup> (deg)	Angle <sup>a</sup> to North (deg)
FNAL → Soudan, MN	731.04 [-0.39]	@FNAL	3.473 [+0.182] <sup>b</sup>	-23.625 [+0.073]
		@Soudan	3.126 [-0.164]	153.597 [+0.073]
FNAL → Carlsbad, NM	1,748.87 [-0.18]	@FNAL	7.791 [-0.098]	-121.626 [-0.081]
		@Carlsbad	8.009 [+0.120]	48.689 [-0.075]
FNAL → Homestake, SD	1,290 <sup>c</sup>	@FNAL @Homestake		
FNAL → Gran Sasso, It	7,332.89 [-2.82]	@FNAL	35.149 [+0.008]	50.087 [+0.004]
		@Gran Sasso	35.155 [+0.005]	-50.749 [-0.006]
FNAL → Kamioka, Jpn	9,133.63 [-1.87]	@FNAL	45.811 [+0.008]	-35.178 [-0.016]
		@Kamioka	45.828 [+0.026]	32.102 [+0.007]
BNL → Soudan, MN	1,715.25 [-0.87]	@BNL	7.826 [+0.093]	-56.330 [+0.076]
		@Soudan	7.665 [-0.081]	110.081 [+0.076]
BNL → Carlsbad, NM	2,903.08 [-0.20]	@BNL	13.118 [-0.048]	-98.421 [-0.053]
		@Carlsbad	13.239 [+0.065]	62.563 [-0.041]
BNL → Homestake, SD	2,540 <sup>c</sup>	@BNL @Homestake		
BNL → Gran Sasso, It	6,526.73 [-2.30]	@BNL	30.825 [+0.011]	56.812 [+0.002]
		@Gran Sasso	30.830 [+0.001]	-59.240 [-0.010]

<sup>a</sup>positive = north/east ; negative = west.

<sup>b</sup>numbers in [ ] are values of the elliptic Earth minus those of the spherical Earth.

<sup>c</sup>V. Barger, D. Marfatia, K. Whisnant, hep-ph0108090

**Table 5.** Distance between possible locations of the Neutrino Factory and the Far Detectors. Angles at each locations are also given.

## **7 ENGINEERING FEASIBILITY AND SAFETY STUDY FOR LANDD AND OTHER PARTICLE PHYSICS DETECTORS IN THE WIPP UNDERGROUND**

1. Introduction
2. Potential experiments
  - a. Conceptual design. (Design elements related to safety, shafts, boreholes, containment structures) Description of experimental setups (concentrating on size, fluids, containment issues)
  - b. Safety Issues (general underground safety, need for containment and venting systems, potential hazards if these are not accounted for, need for procedures and general safety systems)
3. Safety systems analysis
  - a. Systems in place at the WIPP
  - b. Incorporation of these systems into an experimental facility
  - c. Safety elements resulting from experimental setups. (Includes a discussion of resulting engineering configuration control, development of operating and maintenance procedures, etc)
4. Coordination Engineering: Practical Issues in fielding of experiments underground
  - a. Issues related to fielding of experiments (difficulties of working underground, need for tight control of personnel and equipment, regulatory issues)
  - b. Capabilities existing at WIPP and LANL to support fielding
5. Scope of Work
  - a. Conceptual Engineering Studies and Layouts
  - b. Safety and Risk Assessment
  - c. Practical Issues related to fielding of experiments
6. Schedule and Cost
7. Conclusion

## 7.1 Introduction

While mankind has extracted mineral resources from the earth since time immemorial, the creation of underground space for other purposes is, relatively, very new. The utilization of this space, often by large numbers of the untrained general public, creates unique situations where common methods for ensuring safe and effective operations may be inadequate and ineffective. The mineral extraction industry has developed a number of prescriptive codes and rules to enhance safety in underground mining situations, most of which are based on bitter experience. While these codes and rules in general also apply to other underground applications which are not related to mining, they rarely cover many of the specific and unusual underground space applications now being considered. The Waste Isolation Pilot Plant may be unique in this regard, since it has deep and relevant experience in meeting and exceeding highly prescriptive operational and safety regulatory requirements. Since its inception, the Waste Isolation Pilot Plant has achieved world-wide recognition of its safety culture as applied to unique and demanding underground applications. One unique feature of the WIPP lies in the combination of the safety systems and methods adopted from the mining industry, with those developed by the nuclear industry. This industry has developed rigorous processes for ensuring safe construction and operation of nuclear facilities, and in applying these has established an enviable safety record.

In recent years, the particle physics community has recognized the potential for discovering fundamentally new physics beyond the standard model by siting extraordinarily sensitive particle detectors in deep underground settings. With much reduced background “noise” from cosmic ray induced reactions above ground, these experiments promise to revolutionize our understanding of the universe in which we live. Some of these detector concepts are relatively simple and can be safely designed and operated within the normal envelope of underground operations practiced by the modern mining community. Others, however, contain exotic materials and are of such a size that conventional design and safety practices are stretched even for surface application, let alone the much-more demanding underground environment. Certainly, safe installation and operation of the proposed LANNDD, with tens of thousands of tons of oxygen-displacing liquid argon at cryogenic temperatures, will require significant safety engineering considerations.

This chapter describes the engineering feasibility and conceptual design efforts that will be conducted to evaluate the installation and operation of the LANNDD in an underground setting. While LANNDD could conceptually be sited at any number of underground facilities, we believe that the optimum location (including safety considerations and cost) is at WIPP and that only WIPP has the experience to economically design, evaluate, permit, construct, and operate an underground LANNDD meeting acceptable operational and safety standards. The recent fires from flammable (or other hazardous chemical) shipments through highway tunnels has called into question the advisability of siting physics experiments with a potential for serious safety implications in these types of facilities. Even the Channel Tunnel, with its extreme emphasis on safety, experienced a significant fire. Siting a facility such as a LANNDD in any deep mine with limited egress capability (for both egress time and evacuation options), will be costly and will likely depend on the use of refuge rooms, an undesirable and problematic solution

The extraordinary physics potential of LANNDD (charge, mass and directionality) does not demand a deep setting. Overburden depths of 1000-2000 meters of water equivalent (mwe), which can be achieved at the WIPP, provide adequate attenuation of cosmic ray generated muons

and subsequent fast neutrons. Indeed, siting of LANNDD at WIPP will derive additional benefit, due to the extremely low radon production potential of the host rock.

Siting a facility such as the LANND in a hard-rock location, where mining is difficult and slow, could add significantly to the overall cost of supplying suitable egress and suitable venting systems in the event of major disruptions of containment. By contrast, the low cost of mining, shaft installation, and material removal in a salt mine provides a cost effective solution to the safety implications posed by installation and operation of LANNDD in an underground environment. Multiple emergency air dumps and sources, along with multiple egress options, can be simply created at reasonable cost. This chapter describes the feasibility study that will be conducted and lays out milestones for delivering conceptual designs for a variety of detector installations. These will be accompanied by preliminary safety analyses and cost estimates, both of which will be discussed in detail. Development of a detailed design (Title II) for LANNDD at WIPP is not proposed.

The WIPP facility has a long history of dedication to safe operations. Indeed, it can credibly claim to be the safest underground operation in the US today. It has won numerous safety awards, and continues to be recognized for its safety culture around the world. Application of this culture to LANNDD is an exciting opportunity for both WIPP and the physics community.

## **7.2 Potential Experiments**

Two types of detector have been suggested for the Carlsbad site, these being a 50 kT magnetized Fe tracking detector and a 70 kT liquid argon magnetized detector. Conceptually either, or both of these detectors would be located at the current WIPP horizon of 655 m bgs, and would include necessary underground space for control, operation and maintenance of the detectors. This experimental area would, in concept, maintain access to the WIPP storage areas for additional egress and safety reasons, but would be isolated and would maintain a separate means of access from the surface. The engineering and safety issues that would be addressed in a feasibility study of these detectors are discussed in the following sections.

### **7.2.1 Magnetized Fe Detector**

In concept this detector would consist of a stack of alternating magnetized iron plates separated by active detectors with nominal dimensions of 8 m high x 8 m wide x 150 m (500m??) long. The detector would be housed in a tunnel of sufficient size to allow access to the detector, and oriented so as to point towards the site of a neutrino factory. This site might be FNAL, BNL, CERN or JHF. The requirement for the detector to point towards the factory site will require it to be oriented toward that site in the horizontal plane, and decline at angles to the horizontal which would be  $7.8^\circ$  for a factory at FNAL, or up to  $39.5^\circ$  for one at CERN.

#### *Engineering Issues*

Conceptually the tunnel required to house this detector might need to be about 10 m x 10 m in section to allow access to the detector for maintenance. Mining such a tunnel in salt at the WIPP horizon should not be a problem, provided the required grade is less than about 15% (or about  $8.5^\circ$ ). The expected span of the tunnel of the order of 10 m is similar to the current span in the WIPP storage rooms. The height of nominally 10 m is larger than the current excavations, which have a height of the order of 4 m, but this should be achievable with careful design. Careful

design of roof control systems would also be needed for a tunnel crossing clay and anhydrite partings.

A tunnel at a steeper grade, such as that needed for a CERN detector would be much more difficult to mine, equip and maintain, since normal mining and underground transport equipment cannot operate on these steep grades, and special equipment would be needed. In addition emplacing the detector, and physically restraining it, at steep grades would be challenging: some form of sled and hoist arrangement would need to be designed. For a shallower grade installation would be more straightforward, though some issues would need to be resolved in the methods of handling large (8 m x 8 m) plates in the confines of the shafts and the underground.

Engineering issues to be addresses during the feasibility study would include:

- Design of the tunnel section to accommodate creep closure of the section
- Design of tunnel mining pattern to aid in roof control
- Design of roof and strata control and maintenance systems
- Special considerations for a high angle tunnel (if needed)
- Installation, restraint (if needed) and maintenance procedures for the detector.

#### *Safety Issues*

For a low angle (FNAL) tunnel, the design and layout is a relatively minor deviation from current designs, so safety issues are well understood, and mostly concern strata control during mining and operation. Installation of large and heavy elements of the detector in the confined shaft and underground space will also bring safety issues, but these are in the realms of normal industrial safety practices.

A high angle tunnel, such as would be needed to point towards CERN for example, involves more complex issues of safety. Mining such a tunnel would be most easily achieved using drill and blast techniques – alternatively the tunnel would have to be mined in a series of benches. Each of these methods brings special safety issues during construction. As noted above, the emplacement of heavy detector elements would be quite challenging in a high angle tunnel and would involve potentially hazardous working conditions, as would maintenance of the detector during operation.

All of these issues will be reviewed in detail in the feasibility study. There are no special safety concerns related to the detector itself, save those having to do with physical restraint in a high angle detector.

### **7.2.2 Liquid Argon Detector**

Conceptually this detector would involve a tank containing 70 kT of liquid argon. This mass of liquid argon translates into about 50,000 m<sup>3</sup>, or a cylindrical container about 40 m (130 ft) in diameter and 40 m (130 ft) high. The argon container will be surrounded by a solenoid coil and a cryostat.

### *Engineering Issues*

The conceptual design for this detector would call for a large cavity being mined at, or close to, the WIPP horizon. This cavity would, in concept, be a vertical cylinder that, although it will be large, represents the most stable shape for the WIPP conditions that will minimize horizontal creep closure. The roof and floor of this cavity will show more pronounced effects of creep, and the possibility of slabbing and roof falls. The potential for these can be reduced by effective design of the roof and floor, and by appropriate use of support elements. Examples of effective design would be to use an arched roof, and to place the cavity vertically so that major parting planes (clay and anhydrite seams) are avoided at critical locations in the cavity.

Other engineering issues would be related to access requirements for the large detector and safety elements associated with the need to control unintended releases of argon gas. Engineering items to be evaluated in the feasibility study would include:

- Location of the cavity in the salt section so as to avoid partings at critical locations
- Design of the roof section so as to optimize stability
- Design of the floor, and the supports for the argon chamber, so as to minimize the effects of creep.
- Conceptual design of mining approach and mucking systems to develop the cavity at reasonable cost and in a reasonable time.
- Development of roof and strata control systems..

### *Safety Issues*

The major safety issues associated with this detector are centered on the containment of the liquid argon, and the possibility of leakage or of a catastrophic release. The cavity and detector design will need to address this issue through the use of safety shields to mitigate the effects of unexpected ground movement, and through the design of containment systems. Containment design would start with the location of the detector: by situating it below the working horizon the potential inundation of working areas with heavier than air argon would be minimized. This would be combined with passive collection systems at the base of the structure, and venting systems associated with boreholes to the surface.

Other safety issues would revolve around the control of the ground surrounding the argon detector, and the normal industrial hazards associated with constructing and maintaining such a large structure. All of these would be addressed as part of the feasibility study.

### **7.2.3 Ancillary Systems**

Any detector of the size and complexity of those described here will bring with it various ancillary systems. These might include power, ventilation, cooling systems and various maintenance items. In addition these large detectors will need to be constructed underground, and all components will need to be brought in from the surface. Experimenters and support personnel will need access to the detectors and associated instrumentation and computer facilities, and maintenance personnel will need shop facilities to effect repairs.

Some of these systems may be deployed on the surface, but most will need to be in the underground. Access will likely include a dedicated shaft for removal of salt during mining, for bringing components and supplies into the underground during construction, and for access



during operations. Underground facilities for ancillary systems are expected to be routine in terms of construction and maintenance, since they will by and large be of similar designs to current openings. However the scope and extent of these facilities will be evaluated as part of the feasibility study.

### **7.3 Safety Systems**

A significant advantage of WIPP as a host for these experiments lies in the existing culture of safety at this facility, which is more stringent than other mining settings. Many safety systems and processes are already in place and available for adoption by the physics community.

#### **7.3.1 Safety at WIPP**

The WIPP has in place institutional programs that provide an inclusive strategy to support safe operation of the WIPP facility. These programs fulfill the objectives of protection of human health and the environment; emergency preparedness; and cost effective project management.

These programs create a comprehensive safety culture based on several formal processes. These processes identify safeguards that:

- control facility design and changes thereto;
- apply appropriate design classifications, codes, and standards;
- manage configuration control, document control, and quality assurance;
- ensure adequate conduct of operations, engineering, and maintenance; and
- control material usage, operating and maintenance procedures, training and qualification programs, and emergency plans and procedures.

The application of these programs to a unique and complex facility such as the LANND will provide a high degree of assurance that the facility can be built and operated in a safe and effective manner. In addition to the beneficial safety improvements, a properly managed and controlled experimental facility will have a much greater probability of meeting stringent operation specifications and thus achieving research objectives.

#### **7.3.2 Safety Analysis**

The WIPP safety is based on:

- determination of the adequacy of the design basis and the application of appropriate engineering codes, standards, and quality assurance requirements;
- selection and control of principle design and safety criteria;
- determination of necessary Technical Safety Requirements (TSRs);
- controlled conduct of operations; and
- institutional control of safety assurance.

This involves a number of steps, of which one is a hazard and operability study (HAZOP), culminating in a Safety Analysis Report (SAR). While these processes are generally understood within the nuclear community, they may be unfamiliar to others and hence are described in following sections.

### *HAZOP Process*

A hazard and operability study is a systematic method of identifying process hazards and potential operating problems by investigating process deviations. Largely qualitative techniques are used to pinpoint weaknesses in design or operation of the facility that could lead to accidents. The hazard analysis process identifies and categorizes accident scenarios that may be internally initiated, externally initiated, or due to natural phenomena. Accident analyses at WIPP currently utilize applicable Rules, DOE Orders, standards, and guidance. These are directed almost entirely at radiological safety and it will be necessary to find (and possibly develop) similar standards for an experimental facility such as the LANNDD.

In evaluating hypothetical accidents, a level of conservatism is used in the safety analysis assumptions in order to provide potential consequences that are overestimated rather than underestimated. The level of conservatism chosen should bound the full range of possible scenarios. Then, when system variability is taken into account, there is reasonable assurance that the:

- safety envelope of the facility is defined;
- design of the facility is adequate in response to the accident scenarios analyzed; and
- TSRs assigned provide adequate protection of human health and the environment.

It will be necessary to choose appropriate levels of conservatism for the facilities evaluated since those used for WIPP as a nuclear waste repository may not be suitable.

### *SAR*

A safety analysis is a documented process to 1) provide systematic identification of hazards; 2) describe and analyze the adequacy of the measures taken to eliminate, control, or mitigate identified hazards; and 3) analyze and evaluate potential accidents and their associated risks. A Safety Analysis Report (SAR) is a document that describes the adequacy of the safety analysis to ensure that the facility can be constructed, operated, maintained, and shutdown safely and in compliance with applicable laws and regulations. A "preliminary" SAR generally refers to a facility in the design, construction, or pre-operational stage while a "final" SAR indicates that the facility is operating.

A SAR generally contains sections which describe the facility being evaluated, the general design and method of operation of the facility, and the HAZOP and accident analyses performed for that facility. It then describes the necessary measures to ensure the safe operation of the facility. It is proposed to prepare a Preliminary Safety Analysis Report (PSAR) for the experimental facilities. Parts of this PSAR may be applicable to these facilities no matter where they might be constructed, but since the PSAR will obviously build on the extensive WIPP foundation already in place, it will not be generally applicable to any other site.

Technical Safety Requirements (TSRs) define the conditions, safe boundaries, and management and administrative controls necessary to ensure the safe operation of the facility. Established policies and procedures must be in place ensuring normal and emergency procedures are implemented, adequate directions have been provided to personnel concerning actions to be taken in a potential accident environment, and adequate procedures are available for follow-up response. They ensure that facility operations are conducted by trained and certified/qualified

personnel in a planned and controlled manner. And finally, they ensure that hazards remain within the bounds assumed or that deviations from the assumed hazard bounds are at an acceptably low frequency. TSRs will likely play a large role in the operation of a large and complex facility such as the LANNDD where accident consequences are significant and many people who use the facility are likely to be unaware of the variety of accident consequences possible in an underground environment.

Recent examples illustrate the importance of such an intensive safety analysis and the controls derived from it. The Kaprun tunnel fire, which claimed 155 lives, was apparently caused by a faulty space heater, installed illegally, adjacent to hydraulic pipes. The accident resulted from a series of controllable events. The steepness of the tunnel and the complete lack of evacuation facilities then exacerbated the consequences. This situation should not be thought unique. A recently completed 24.5 km long road tunnel has no automatic alarms or escape routes. The recent fire in the St Gotthard tunnel left at least 11 dead in spite of fire detectors, phone and push button alarms, video monitoring, and a parallel escape tunnel. Available safety systems worked well and the alert was sounded within 4 minutes but if truck drivers familiar with the tunnel had not helped others to safety, the death toll might have been much higher.

### **7.3.3 Application to Experimental Facilities at WIPP**

The general approach described above will be used to prepare a PSAR. Initially this document will be rather general and it will need to be revised as the design of the facility progresses. The first version however should provide fundamental system safety requirements and identify aspects requiring further consideration at a later date. Once a reasonably complete conceptual design is available a HAZOP will be performed. The identification and use of appropriate available WIPP resources (such as policies, processes, and procedures) will greatly speed the completion of the PSAR.

This systematic approach to hazard analysis will be conducted by a leader knowledgeable in the HAZOP methodology and the HAZOP team will consist of personnel from various disciplines familiar with the intended design and operation of the facility. The HAZOP team will identify deviations from the intended design and operation of the facility that could result in worker injury or fatality, slowdown or shutdown of operations, or an abnormal release of contained materials.

The HAZOP team will attempt to assign a qualitative consequence and frequency ranking for each deviation. A hazard evaluation ranking mechanism will utilize the frequency and most significant consequences to separate the low-risk hazards from high-risk hazards. This will allow resources to be efficiently directed during later design activities. Based on this ranking approach HAZOP deviations whose combined hazard rank are identified to be of moderate or high risk may be selected for quantitative analysis to identify higher level safety requirements.

The conceptual design will be summarized in the PSAR along with the results of the HAZOP. System specifications and TSRs which derive from these will likely be general at this stage but should reasonably define the designs, configurations, processes, procedures, and administrative controls necessary for the safe operation of the facility.

## **7.4 Coordination Engineering: Practical Issues in Fielding Experiments Underground**

### **7.4.1 Issues related to fielding of experiments**

The fielding of complex, large-scale experiments or tests in diversely regulated, multi-use facilities is always challenging and unique to each test, facility and participant situation. Only a handful of programs and facilities worldwide have undertaken this type of integrated technical and logistical challenge, and few organizations have the experience and capability to safely and successfully field these types of experimental programs, especially in an underground environment.

During the detailed planning and implementation phases of the LANNDD program at WIPP, a diverse range of issues will need to be addressed by the integrated team of investigators, test and facility designers, constructors and facility operators. These issues must be identified at this feasibility stage, and a methodology for addressing them developed. Major areas of focus and examples of the associated issues include:

- Facility owner (DOE) interface
  - o Facility clearances, site and underground access and accountability, escort requirements, official site representation, liability assignments
- User's basic knowledge and sophistication
  - o Underground and surface facility operations knowledge, safety and security sensitivity
- Training requirements for access and function authorization
  - o Cross-matrix training required by external organization(s), facility operators, facility owners, and applicable local, state and federal regulatory agencies
- Work Authorization
  - o Facility operations interface, potential union issues, safety reviews and controls, document control
- Logistics Support
  - o Transportation, accommodations, remote-site issues, communication infrastructure

In addition to facility-driven issues and interface requirements, investigators must address several key issues, unique to the underground environment, regarding the fielding of their experiments. Most of these issues relate to the complexity of mapping experimental requirements against facility infrastructure (facilities, utilities, operations and maintenance support and reliability, data collection and access). The integration of testing requirements and responsibilities with facility operations requirements and responsibilities is a critical, but often difficult and ignored planning requisite, as is the need to separate test preferences and enhancements from actual requirements. The subsequent translation of test requirements to design, construction and operation requirements, the trade-off and cost analyses for identified options, and the assessment of impacts on experiments due to the selection of alternatives are all crucial integration challenges.

Often overlooked in planning large, complex field experiments which require multiple organizational interfaces is the development and strict adherence to a change control system that fairly and equitably represents operations and experimental requirements and ensures that unilateral changes do not occur. At the same time it must be recognized that field or test conditions often require rapid decisions to be made on modifications or adjustments, so a field-

based control system, which allows rapid response to conditions, also is essential. The WIPP change control system, with elements from both the nuclear and mining industries, is uniquely suited to deal with this situation.

The initial phase (engineering feasibility and conceptual design) of the work proposed here will only require limited scoping of field requirements and initial, high-level definition of interface requirements and testing logistics. It is most critical, however, at this stage to establish, and clearly utilize, interface mechanisms and organizations. These will initially (at high level, low detail) and subsequently (at low level, high detail) provide on-site representation in logistics planning and test organization for the design, construction, and facility operation organizations. Establishing this technical liaison and on-site coordination role in the early phase will insure effective interface control and technical test implementation later.

During this project phase, the WIPP organizations will provide a focused support function to work with investigators and conceptual designers to define and translate high-level requirements and safety considerations for fielding selected experiments in the underground. This function will be expanded in later planning and implementation phases to provide on-site support for investigators in scoping design and operations, and in formal planning.

#### **7.4.2 Existing capabilities at LANL and WIPP to support field experimentation**

The WIPP team of contractors and the existing facility infrastructure is uniquely qualified and experienced in fielding geotechnical experiments in the underground.

Experience gained over the past 20 years on the performance assessment experiments conducted at the WIPP provide invaluable experience for the planning and scheduling of resources in an efficient manner, so as to save time and money during both the construction phase and the operating phase. The question of when and how to excavate specialized opening can be readily addressed by the WIPP mine engineering staff, and is addressed elsewhere in this proposal. The WIPP has developed many excavation and test-support plans for efficient and timely development of panels and drifts for waste emplacement and geotechnical testing.

The WIPP has a team of certified Industrial Hygienists that will evaluate the experimental program and suggest proactive design features that will ensure the highest level of safety to protect the scientists and the expensive experimental equipment. This team knows the regulations and limits, ensuring that scientists will be able to incorporate the right controls and safety features to operate within the limits identified in the PSAR. In addition, the WIPP has a supporting work control organization that will help in the execution of the construction process.

Los Alamos National Laboratory (LANL) Carlsbad Operations brings the dual expertise of having a long history of active nuclear and astro-physics research, coupled with and over 50 years of practical expertise in planning and managing the fielding of complex underground and atmospheric tests in both weapons and repository science programs. The WIPP-based LANL team will have access to, and will utilize the extensive physics expertise in various technical divisions of the national laboratory, to assist the WIPP-based LANL support team in defining test requirements and translating these requirements into design and operations systems and interfaces.

Los Alamos will provide unique science-oriented engineering and logistics support modeled after the successful Nevada Test Site Program. At the NTS, LANL has provided lead management and engineering field support for all nuclear weapons tests since 1951. In addition, Los Alamos has been the organizational lead for planning and fielding surface and underground testing and site characterization at the Yucca Mountain project since 1988. The current test program manager at Yucca Mountain from 1989 to 1998 is the resident manager for LANL's WIPP organization in Carlsbad, and brings extensive personal management experience in fielding major test programs.

LANL's unparalleled experience in field test management and logistics coordination, coupled with the WIPP MOC's site-specific expertise in testing programs performed underground at WIPP, provides world-class capability for test planning, facility design, and implementation.

## **7.5 Scope of Work**

### **7.5.1 Conceptual Engineering Studies and Layouts**

#### *Scope of Work*

The activities to be performed in this phase of the feasibility study will be directed towards the preparation of a Conceptual Underground Design Report for the proposed physics experiments. This will involve initially a preliminary evaluation of the needs for the different experiments, in terms of the excavations required for the main experiment (liquid argon tank and/or iron detector), as well as those for ancillary equipment, access, and services. These design requirements will fall into two broad categories: those related to the experimental facilities themselves and those related to the utilization of underground space. The former will be determined in close consultation with the experimenters. Following development of the experimental needs, the conceptual design team will interact with the safety assessment personnel and WIPP operations to evaluate the latter in terms of risk containment, health and safety requirements, and operations. These additional needs might include, for example, the development of separate access, venting systems, ventilation, and power.

At this point the draft Conceptual Underground Design Report will be prepared. This report will contain the fundamental performance specifications for the experimental facilities, which will be used to establish preliminary requirements for the operational and safety standards. This report will form the basis for a program design review to confirm the general adequacy of the proposed specifications and standards.

This draft report will then form the base for more detailed design activities. For example, it will be used to determine the best stratigraphic horizon for the various facilities, which then forms the basis for preliminary stability and ground support calculations. From these studies it will then be possible to refine layouts, and to prepare preliminary estimates for excavation and support costs. These studies will also feed into the design of experimental facilities and how they relate and interact with the underground environment. Regular interaction between the various design teams will be vital to the success of this exercise and specific allocations of time have been made for this purpose.

When these studies are complete, the draft Conceptual Underground Design Report will be revised. It will then be reviewed with the experimental team, safety, and operations and adjustments will be made as needed. The agreed conceptual design will be used as a basis for determining the expected feasibility, cost and schedule for construction. The draft report will then be revised to include these elements and will be issued in final form.

#### *Deliverables*

The draft version of the Conceptual Underground Design Report will be developed, maintained, and presented in electronic format. The report will include drawings sufficient to permit a preliminary estimate of the cost and time necessary to construct the underground facility and any interfaces to the experimental installations.

The final Conceptual Underground Design Report will be prepared in both electronic and hard copy versions. The report will detail the underlying basis for the conceptual design, necessary supporting calculations, safety and operational analyses, and estimated costs and schedules.

## **7.6 Safety and Risk Assessment (WTS)**

#### *Scope of Work*

WIPP will prepare a preliminary Safety Analysis Report for the proposed physics experiments to be performed underground at WIPP. This SAR will be based on conceptual designs for both the experimental installations and the underground configuration selected to house them. The work will consist of several phases.

The first phase will essentially consist of oversight and review of the initial conceptual design activities and determination of fundamental risk elements and parameters. Once preliminary conceptual designs and specifications are available, a HAZOP will be performed to identify those design parameters that most impact facility design and operation. Because the design is still conceptual and broad in nature, it may not be possible to do more than identify the nature of processes and procedures necessary during the detailed design and operation periods for the facility. This phase will require about 500 hours of exempt time.

Once a complete conceptual design is available the second phase will be performed. The second phase will consist of a comprehensive HAZOP and revision of the preliminary SAR. The HAZOP will include several members from outside the design team in order to ensure that an adequate degree of independent opinion is available. Any impacts on WIPP repository operations will be identified but the WIPP SAR will not be modified. This phase will require about 1200 hours of exempt time.

The third phase will be a comprehensive review of the final conceptual designs and such revisions of the preliminary SAR as may be necessary. At the completion of this stage the Preliminary SAR should have identified all significant design requirements. Most operational and administrative TSRs should be identified but it is likely that their specific detail cannot be specified until more detailed designs are available. This phase will require about 300 exempt hours.

This work will also require about 400 hours of non-exempt time. This is associated primarily with secretarial and administrative activities. The work will also require about 400 hours of management and supervision time. All work will be performed using the appropriate WIPP procedures and standards.

#### *Deliverables*

The phase one and two drafts of the Preliminary SAR will be developed, maintained, and presented in electronic format. The final Preliminary SAR will be prepared in both electronic and hard copy versions. Both will be delivered concurrently with the Conceptual Underground Design Report.

### **7.7 Coordination Engineering: Practical Issues in Fielding Experiments**

#### *Scope of Work*

WIPP will develop and then initiate a change control system that fairly and equitably represents operations and experimental requirements and ensures that unilateral changes do not occur. This change control system will be designed to facilitate rapid decision making on modifications or adjustments. WIPP will also propose a field-based control system, which will allow rapid response to conditions during construction. Both the Conceptual Underground Design Report and the SAR will be developed using this change control process.

The initial phase (engineering feasibility and conceptual design) of the work proposed here will only require limited scoping of field requirements and initial, high-level definition of interface requirements and testing logistics. During this project phase, the WIPP organizations will provide a focused support function to work with investigators and conceptual designers to define and translate high-level requirements and safety considerations for fielding selected experiments in the underground. This function must be expanded in later planning and implementation phases (not proposed here) to provide on-site support for investigators in scoping design and operations, and in formal planning.

#### *Deliverables*

A Facility Operations Interface Report will be prepared that presents a recommended change control system. It will include analyses of potential union issues, safety reviews/controls, document control, and work authorization. It will also make recommendations for consideration during detailed design and construction on logistics support, transportation, accommodations, remote-site issues, and communication infrastructure

### **7.8 Schedule and Cost**

#### **Budget for Feasibility Study and Conceptual Engineering**

<b>Labor</b>	<b>Rate</b>	<b>Hours</b>	<b>Cost</b>
Principal	\$150.00	160	\$24,000
Senior Engineer	\$100.00	700	\$70,000
Project Engineer	\$75.00	1040	\$78,000



Staff Engineer	\$65.00	1040	\$67,600
Drafting	\$55.00	320	\$17,600
Secretarial	\$45.00	160	\$7,200
subtotal			\$264,400

**Materials** \$10,000

**Travel**

Assume: 2 x 5-day trips Denver - Los Angeles.

2 x 5-day trips Denver-Carlsbad			
Per Diem (20 days)	\$145.00	20	\$2,900.00
Airfares (4 fares)	\$900.00	4	\$3,600.00
sub-total			\$6,500.00

Sub-total			\$280,900.00
NM Tax	5.75%		\$16,151.75

**Total for Conceptual Engineering Studies and Layouts \$297,051.75**

**Budget for Safety System Analysis**

Labor

Exempt: 2000 hrs @ Senior Engineer*	\$123,960.00
Non-exempt: 400 hrs @ Secretary*	\$ 7,888.00
Supervision 400 hrs @ Line Manager*	<u>\$ 30,440.00</u>
sub-total	\$162,288.00

Materials

Office	sub-total **	\$ 1,000.00
--------	--------------	-------------

Travel

Assume two 5-day trips Carlsbad - Los Angeles.	
Personal 10 days @ \$145 **	\$ 1,450.00
Airfares 2 fares @ \$900 **	<u>\$ 1,800.00</u>
sub-total	\$ 3,250.00

Overhead, Fee, Tax, Miscellaneous

sub-total	\$166,538.00
Fee @6.8%	\$11,325.00
Tax @5.75%	\$ 9,576.00

**Subtotal for Safety Systems Analysis \$187,439.00**

Notes: \* Rates used are:

- Sr. Engineer \$61.98
- Secretary \$19.72

- Line Manager \$76.10
- \*\*\* 5.75% Tax and 6.8% Fee apply to cost of labor, materials, and travel. Overhead applies to labor cost only and is already included in given rates.

**Budget for Coordination Engineering**

Labor		
Technical Staff – Carlsbad	80 Hrs	\$10,000
Technical Staff – Los Alamos	60 Hrs	\$7,500
Sec/Admin Staff – Carlsbad	80 Hrs	<u>\$4,000</u>
Subtotal	\$21,500	
Travel		
Two 5-day trips: Carlsbad/Los Alamos		\$1,500
To Los Angeles, CA		
Expenses		
Airfare (\$800/trip x 4 man-trips)		\$3,200
<b>Subtotal for Coordination Engineering</b>		<b>\$26,200</b>

**7.9 Conclusion**

The WIPP facility has a long history of dedication to safe operations. Indeed, it can credibly claim to be the safest underground operation in the US today. It has won numerous safety awards, and continues to be recognized for its safety culture around the world. Application of this culture to LANNDD is an exciting opportunity for both WIPP and the physics community.

DOE recently decided to formally promote use of the WIPP for research purposes unrelated to its prime mission of waste disposal. In October of 2000, former Secretary of Energy, Bill Richardson designated the Carlsbad Office as a "Field" Office. This designation allowed WIPP to offer its mine operations infrastructure and space in the underground to researchers requiring a deep underground setting with dry conditions and very low levels of naturally occurring radioactive materials.

Several other particle physics detectors of modest scale are currently being developed for installation in WIPP. However, their size and scale do not warrant the depth of analysis that will be required for large, complex and inherently hazardous detectors such as LANNDD. However, even these room-scale experiments using passive materials are being subjected to analyses and safety planning as part of WIPP’s inherent safety culture. The proposed LANNDD and other neutrino factory detectors will demand substantially more analysis and planning. The proposed effort described in the preceding sections represents an important first step towards realizing the development of large underground physics detectors here in the US. WIPP is proud to contribute its facility and expertise in this endeavor.

## References

1. [ref\_RayDavis] R. Davis Jr. et al., Proc. 4th Int. Solar Neutrino Conference, ed. W. Hampel, MPIK Heidelberg, (1997).
2. [ref\_muRing] N. Holtkamp and D. Finley, ed., *A Feasibility Study of a Neutrino Source Based on a Muon Storage Ring*, [http://www.fnal.gov/projects/muon\\_collider/nu-factory/nu-factory.html](http://www.fnal.gov/projects/muon_collider/nu-factory/nu-factory.html), (2000). S. Geer and H. Schellman, ed., *Physics at a Neutrino Factory*, [http://www.fnal.gov/projects/muon\\_collider/nu/study/study.html](http://www.fnal.gov/projects/muon_collider/nu/study/study.html) (2000).
3. [ref\_he6Ring]
4. [ref\_piRing]
5. [ref\_SuperK] J.N. Abdurashitov et al., Proc. 4th Int. Solar Neutrino Conference, ed. W. Hampel, MPIK Heidelberg (1997). Y. Fukuda et al., Phys. Lett. B **335**, 237 (1994). Y. Fukuda et al., Phys. Lett. B **433**, 9 (1998). F. Fukuda et al., *Tau Neutrino Favored over Sterile Neutrinos in Atmospheric Muon Neutrino Oscillations* (2000), hep-ex/0009001.
6. [ref\_SnowmassM1] K.McDonald and A. Sessler, Report from The Snowmass 2001 Working Group M1: Muon Based Accelerators.
7. [ref\_Pontecorvo] K. Zuber, *On the Physics of Massive Neutrinos* (1998), hep-ph/9811267.
8. [ref\_MSW]
9. [ref\_MNS]
10. [ref\_CP]
11. [ref\_BBM] JF Beacom, RN Boyd, A Mezzacappa, Phys. Rev. Lett. **85** (2000) 3568.
12. [ref\_FHM] GM Fuller, WC Haxton, GC McLaughlin, Phys. Rev. **D59** (1999) 085005.
13. [ref\_Smith1] PF Smith, Astroparticle Phys. **8** (1997) 27. DB Cline et al., Phys. Rev. **D50** (1994) 720. S.E.Woosley et al., Ap. J. **356**, 272 (1990).
14. [ref\_Smith2] PF Smith, Astroparticle Phys. (2001).
15. [ref\_SNO] B. Schwarzschild, *Novel Heavy-Water Detector Unveils the Missing Solar Neutrino*, *Physics Today* **54-8**, 13 (2001).
16. [ref\_SNDighe] Dighe and Smirnov, Phys. Rev. **D62** (2000) 033007.
17. [ref\_CHORUS1] E. Eskut et al., *The CHORUS experiment to search for  $\nu_\mu$   $\rightarrow$   $\nu_\tau$  oscillation*, Nucl. Instr. and Meth. in Phys. Res. A **401** (1997) 7-44.
18. [ref\_CHORUS2] The CHORUS Collaboration, *New results on the  $\nu_\mu$   $\rightarrow$   $\nu_\tau$  oscillation search with the CHORUS detector* (1999), hep-ex/9907015.
19. [ref\_Garren] D.B. Cline et al., *Physics and Detector Consideration with a Bow-Tie Storage Ring and Multiple Neutrino Detectors*, Presented at the 5th Int. Conf. Sponsored by UCLA on Physics Potential and Development of  $\mu^+\mu^-$  Colliders (San Francisco, Dec. 15-17, 1998).
20. [ref\_nuCrossn] R. Gandhi et al., *Neutrino Interactions at Ultrahigh Energies* (1998), hep-ph/9807264.
21. [ref\_sensitivity]
22. [ref\_Nuphysics] E. Akhmedov, *Neutrino Physics* (2000), hep-ph/0001264.
23. [ref\_Bfibers] Applied scintillation Technologies, Harlow, UK, data sheets.
24. [ref\_Lifibers] M Bliss et al., Proc. SPIE **2551** (1995) 108.
25. [ref\_ICARUS] ICARUS Collaboration, «*ICARUS-II. A Second-Generation Proton Decay Experiment and Neutrino Observatory at the Gran Sasso Laboratory*», Proposal Vol. I & II, LNGS-94/99, 1994.

26. [ref\_ICARUS2] ICARUS Collaboration, “A first 600 ton ICARUS Detector Installed at the Gran Sasso Laboratory”, Addendum to proposal, LNGS-95/10 (1995).
27. [ref\_ICARUS3] F. Arneodo et al. [ICARUS and NOE Collaboration], “ICANOE: *Imagine and Calorimetric Neutrino Oscillation Experiment*”, LNGS-P21/99, INFN/AE-99-17, CERN/SPSC 99-25, SPSC/p314; see also A. Rubbia [ICARUS Collaboration], hep-ex/0001052. Updated information can be found at <http://penometh/cern/ch>.
28. [ref\_OPERA] OPERA Collaboration, *OPERA Progress Report*, LNGS-LOI 19/99, <http://www.cern.ch/opera/documents.html>.
- [ref\_MINOS] The MINOS Collaboration, *The MINOS Detectors Technical Design Report* NuMI-L-337, [http://www.hep.anl.gov/ndk/hypertext/minos\\_tdr.html](http://www.hep.anl.gov/ndk/hypertext/minos_tdr.html) (1998). <sup>1</sup>A.O. Bazarko, *MiniBooNE: Status of the Booster Neutrino Experiment* (2000), hep-ex/0009056.
29. [ref\_Geer]
30. [ref\_UNL] Los Alamos National Laboratory et al., *Prospects for an Underground Laboratory in Carlsbad, NM* (2001), <http://www.wipp.carlsbad.nm.us>.
31. [ref\_UNL2] Battelle, *Environmental Assessment for Conducting Astrophysics and Other Basic Science Experiments at the WIPP Site*, Dept. of Energy Carlsbad Field Office (2000).
32. [ref\_UNL2] F. P. Calaprice et al., *Report on the Technical Evaluation of Underground Laboratory Sites* (2001), <http://www.sns.ias.edu/~jnb/Laboratory/evaluation.html>.
33. [ref\_UNL3] Boyd et al., Nucl. Instr. and Meth. in Phys. Res. A **399**, 269 (1997).

1

<sup>1</sup>T. Kirsten, Talk presented at TAUP97, Gran Sasso (1997).

1

<sup>1</sup>M. Spurio et al., *Low energy atmospheric  $\mu$  in MACRO* (1998), hep-ex/9808001.

<sup>1</sup>F. Boehm et al., *Search for Neutrino Oscillations at the Palo Verde Nuclear Reactors* (1999), hep-ex/9912050.

<sup>1</sup>C. Athanassopoulos et al., *Phys. Rev. Lett.* **77**, 3082 (1996).

<sup>1</sup>K. Eitel et al., *Latest Results of the KARMEN2 Experiment* (2000), hep-ex/0008002.

1

T. Ishida et al., *The First Results of K2K long-baseline Neutrino Oscillation Experiment* (2000), hep-ex/0008047.<sup>1</sup>

<sup>1</sup>P. Renton, *Electroweak Interactions*, Cambridge Univ. Press, Cambridge, (1990).

1

<sup>1</sup>B.M. Gallager and M.C. Goodman, *Neutrino Cross Sections* (1995), NuMI-112.

<sup>1</sup>A. Weinstein, *Tau Electroweak Couplings* (1999), hep-ex/9911002.

<sup>1</sup>E. Eskut et al., *Phys. Lett. B* **434**, 205 (1998).

<sup>1</sup>D.A. Harris and A. Para, *Neutrino Oscillation Appearance Experiment using Nuclear Emulsion and Magnetized Iron* (2000), hep-ex/0001035.

1